Determining Load Characteristics for Transient Performance Volume 2: Load-Model Guidelines

EL-850, Volume 2 Research Project 849-1

Final Report, March 1981

Prepared by

GENERAL ELECTRIC COMPANY
Electric Utility Systems Engineering Department
1 River Road
Schenectady, New York 12345

Authors T. Gentile S. Ihara A. Murdoch N. Simons

Prepared for

Electric Power Research Institute 3412 Hillview Avenue Palo Alto, California 94304

EPRI Project Manager J. V. Mitsche

Power Systems Planning and Operation Program Electrical Systems Division

DISCLAIMER

Portions of this document may be illegible in electronic image products. Images are produced from the best available original document.

ORDERING INFORMATION

Requests for copies of this report should be directed to Research Reports Center (RRC), Box 50490, Palo Alto, CA 94303, (415) 965-4081. There is no charge for reports requested by EPRI member utilities and affiliates, contributing nonmembers, U.S. utility associations, U.S. government agencies (federal, state, and local), media, and foreign organizations with which EPRI has an information exchange agreement. On request, RRC will send a catalog of EPRI reports.



EPRI authorizes the reproduction and distribution of all or any portion of this report and the preparation of any derivative work based on this report, in each case on the condition that any such reproduction, distribution, and preparation shall acknowledge this report and EPRI as the source.

NOTICE

This report was prepared by the organization(s) named below as an account of work sponsored by the Electric Power Research Institute, Inc. (EPRI). Neither EPRI, members of EPRI, the organization(s) named below, nor any person acting on their behalf: (a) makes any warranty or representation, express or implied, with respect to the accuracy, completeness, or usefulness of the information contained in this report, or that the use of any information, apparatus, method, or process disclosed in this report may not infringe privately owned rights; or (b) assumes any liabilities with respect to the use of, or for damages resulting from the use of, any information, apparatus, method, or process disclosed in this report.

Prepared by General Electric Company Schenectady, New York

ABSTRACT

This study evaluated a prototype load modeling procedure developed by the University of Texas at Arlington (UTA) in EPRI project RP849-3. Tests were run on three different power systems to evaluate the procedure's accuracy in modeling the dynamic power response of loads (active and reactive) when subjected to limited excursions of voltage and frequency. In support activities, guidelines were developed for the load modeling procedure, and possible data sources for it were investigated.

The period of performance was September, 1976 to July, 1980. The work accomplished by General Electric is reported in a final report of four volumes, the contents of which are as follows:

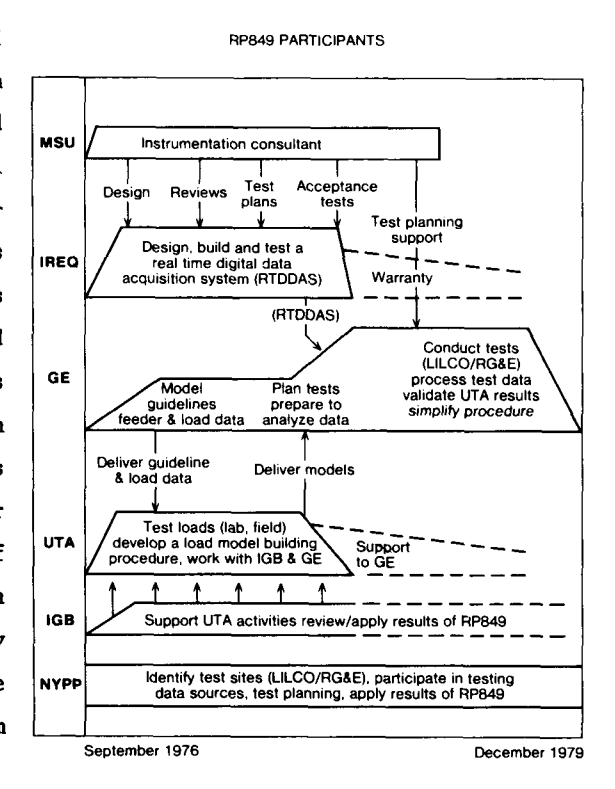
- Volume I: Executive Summary An overview and summary of results are presented. Recommendations are made for the research necessary to develop a production grade load modeling procedure.
- Volume II: Load Model Guidelines
 Guidelines are developed for a load modeling procedure. Induction motor
 characteristics and their effect on system stability are examined.
- Volume III: Load Composition Data Analysis Possible data sources for the load modeling procedure are identified and analyzed as to their potential for use in determining the composition of bus load by component. A methodology is proposed.
- Volume IV: Test Data Analysis
 Test results on three power systems are reported and analyzed. An evaluation of the UTA load modeling procedure is made.

EPRI PERSPECTIVE

PROJECT DESCRIPTION

RP849 involved several participants (see figure below) including three major contractors: Institut de Recherche de l'Hydro Quebec (IREQ), General Electric Company (GE), and the University of Texas at Arlington (UTA). This research was performed to better understand and model the dynamic characteristics of power system loads particularly when they are subjected to abnormal voltage or frequency changes. This 48-month effort was the first large-scale research aimed at forming load models as accurate as those commonly used for generators and other power system components. A mobile, real-time digital data acquisition system (RTDDAS) was designed, built, and used to record load characteristics in substation tests at Long Island Lighting Company (LILCO) and Rochester Gas and Electric (RG&E).

The four volumes comprising EPRI Final Report EL-850, together with Final Reports EL-849 EPRI EL-851, document the load-model building and testing research performed in RP849. Through this research, significant progress has been made in understanding modeling the dynamic characteristics However, as discussed in of load. EPRI EL-850, many important problems remain to be resolved. research built upon the results of this project should result in a procedure through which utility engineers can significantly improve the accuracy of power system analysis.



SCOPE OF GE WORK

As shown in the figure, the work done by GE was central to the load-modeling research done in RP849. Their overall role was to evaluate the load-model building procedure developed by UTA. This was done by comparing the

responses of utility feeders during staged disturbances to the simulated responses using data describing those feeders. Specifically, the tasks were:

- To illustrate the effect of varying the types of load models used in computer simulations of power systems
- To identify and evaluate the utility data sources required in the load-modeling procedure
- 3. To plan and conduct several power system field tests
- 4. To use the field test results to evaluate the UTA load-modeling procedure performance and to suggest possible improvements if necessary

CONCLUSIONS

As a result of this work, it was found that a load model can be synthesized by combining the characteristics of individual components that make up the load (e.g., air conditioners, pumps, heaters). To construct this load model the user must know the number of each component that is "on" at the time of interest. Typical response characteristics of each of these components are then combined to form a composite model. This procedure is less expensive, more versatile, and more accurate than the use of field tests to measure load response.

As one part of their work, GE identified sources of data used to count what components of load are "on" at any given location and time. Up to this time, these data, which are now being collected by many utilities for load research and other studies, have not been utilized to study power system transient performance.

The discussion of the use of load models in this report, although somewhat oversimplified, does accentuate the importance of modeling loads in computer studies. The treatment of induction motor modeling, its impact on simulation results, and the computer modeling data supplied are substantial contributions to the body of knowledge of computer analysis of power systems.

The extensive work done to test and analyze the model building procedures developed by UTA has identified both the successes and shortcomings of this procedure. The comparison and analysis of predicted and recorded results demonstrate the validity of the principles of this research and emphasize

the limited validity and usefulness of the present modeling procedure. The large reservoir of unique and valuable test data collected has not yet been fully explored. The analyses and recommendations reported here can be used to plan and perform future research.

Follow-on research is needed to correct the inaccuracy that exists in the reactive power and dynamic response characteristics of the load models. The load-model building procedure must also be simplified before it is suitable for routine use by utility engineers.

James V. Mitsche, Project Manager Electrical Systems Division

ACKNOWLEDGMENTS

The authors wish to express their thanks to Dan Carlson of Minnesota Power and Light Company, Tom Frantz of Rochester Gas and Electric Company, Bob Iveson of Electric Power Research Institute (formerly with New York Power Pool), Eric Mc Clelland of New York Power Pool, Gary Paulsen of Montana-Dakota Utilities Company, and Mark Waldron of Long Island Lighting Company for their assistance in planning, conducting and analyzing the tests run in this project as well as providing overall direction for the research.

	,		

CONTENTS

Sect	ion	Page
1	INTRODUCTION	1-1
2	SUMMARY OF GUIDELINES	2-1
3	GENERAL SYSTEM GUIDELINES	3-1
	Transient Stability	3-2
	Dynamic Stability	3-6
4	INDUCTION MOTOR EFFECTS	4-1
	Transient Stability	4-1
	Dynamic Stability	4-9
5	INDUCTION MOTOR PERFORMANCE ANALYSIS	5-1
	Description of the Model	5-1
	Steady-State Results	5-2
	Transient Results	5-8
6	REFERENCES	6-1
APPE	NDIX A PARAMETERS FOR SYSTEM STUDIES	A-1

ILLUSTRATIONS

Figure		Page
3-1	Configuration of the two-machine system used in the guidelines studies	3-2
3-2	Effect on stability of changing active power load models - local and remote generation configurations; reactive power loads modeled as constant impedances	3-3
3-3	Effect on stability of changing reactive power load models - local and remote generation configurations; active power loads modeled as constant currents	3- 5
3-4	Effect on transient stability of excitation system changes relative to changes in the active power load representation .	3-6
3-5	Indication of system dynamic stability in the two-machine system as a function of steady-state load model representation; open-loop transfer function of a change in generator electrical torque for a change in rotor angle for generator 2	3-8
4-1	Effect on transient stability of modeling induction motor dynamics, relative to use of a totally static load model	4-2
4-2	Transient response of three-machine system with 5500 hp motor characteristics, remote generation, 80 millisecond ₂ fault; motor inertia, H=1.0 second; shaft torque = 0.75 w ²	4-4
4-3	Transient response of two-machine system with all static load characteristics (V/V^2) , remote generation, 80 millisecond fault	4-5
4-4	Steady-state and dynamic response of 5500 hp induction motor; active and reactive power versus voltage; dynamic response to a 6 cycle system fault	4-7
4-5	Gain and phase of transfer function, $\Delta P/\Delta V,$ for 5500 hp induction motor	4-11
4-6	Gain and phase of transfer function, $\Delta Q/\Delta V,$ for 5500 hp induction motor	4-12
5-1	Induction motor equivalent circuit in d and q axis representation and synchronously rotating reference frame	5-2
5-2	Air-gap saturation characteristics for the induction motors studied	5-3
5-3	Motor input power versus voltage for 30 hp motor, constant shaft torque	5-6
5-4	Motor input power versus voltage for 30 hp motor, rated torque, ±5% frequency variation	5-6

<u>Figure</u>		Page
5-5	Motor input power versus voltage for 30 hp motor, shaft torque proportional to w	5-6
5-6	Motor input power versus voltage for 30 hp motor, rated torque proportional to ω^2 , $\pm 5\%$ frequency variation	5-6
5-7	Motor input power versus voltage for 5500 hp motor, constant shaft torque	5-7
5-8	Motor input power versus voltage for 5500 hp motor, rated torque, ±5% frequency variation	5-7
5-9	Motor input power versus 2 voltage for 5500 hp motor, shaft torque proportional to w^2	5-7
5-10	Motor input power versus 2 voltage for 5500 hp motor, rated torque proportional to w^2 , $\pm 5\%$ frequency variation	5-7
5-11	System for study of single induction motor transients	5-8
5-12	Transient response for 30 hp motor; single motor to infinite bus system	5-9
5-13	Transient response for 5500 hp motor; with rotor p Ψ terms; single motor to infinite bus system	5-10
5-14	Transient response for 5500 hp motor; without rotor $p\Psi$ terms; single motor to infinite bus system	5-12
5-15	Plot of motor P and Q versus voltage; transient response for 30 hp motor (corresponds to Figure 5-12)	5-13
5-16	Plot of motor P and Q versus voltage; transient response for 5500 hp motor, with rotor pw terms (corresponds to Figure 5-13)	5-14
5-17	Plot of motor P and Q versus voltage; transient response for 5500 hp motor, without rotor pΨ terms (corresponds to Figure 5-14)	5-15

TABLES

<u>Table</u>		Page
4-1	Effect of varying inertia and shaft load characteristics for 5500 hp motor load	4-6
4-2	Effect of neglecting rotor electrical dynamics on transient stability of three-machine system	4-8
4-3	Effects of aggregation using two induction motors on transient stability	4-9
4-4	Transfer functions for 5500 hp induction motor	4-10
4-5	Local mode eigenvalue for two-generator system with load representation varied	4-13
5-1	Induction motor data	5-3
5-2	Induction motor steady-state operating points	5-4

SUMMARY

The overall objective of General Electric's research in the EPRI RP849-1 project was to evaluate, through field tests, the load modeling procedure developed by the University of Texas at Arlington (UTA) in EPRI project RP849-3. The UTA load modeling procedure was used to develop load models for four different load buses on three electric utility systems for different seasons of the year. Extensive field tests at these load buses were conducted to evaluate the load models.

The philosophy implemented in the UTA load modeling procedure is to develop the load characteristics and model for a system bus based on the composition of the system load by component (air conditioning, lighting, etc.) and the voltage and frequency characteristics of those components. When the RP849 research began, it was not certain that sufficient data existed to support such a load modeling procedure. An important part of the General Electric research was to determine the availability and accuracy of data which could be used to synthesize the load composition of a system bus. Subsequently, this data was used as inputs to the UTA procedure to develop load models for the load buses to be tested. The field tests then are being used to not only evaluate the analytical techniques of the UTA load modeling procedure, but also the very load modeling philosophy being attempted.

Early in the overall RP849 project, the EPRI project manager (T. Yau) requested guidance to define the most important characteristics for inclusion in the UTA load component and composite load models. GE provided guidelines for these decisions using transient stability studies with various load models which existed before the RP849 project began. The particular concern was to demonstrate the sensitivity of system performance to various uncertainties in the load model characteristics.

The research and results are summarized here under the three main areas - load model guidelines, load composition data analysis, and load model evaluation.

LOAD MODEL GUIDELINES

Studies were made with a simple 2-machine system to demonstrate the effect of load model characteristics on system transient stability. The measure of stability used in this case was the maximum angle swing between the two machines. The system loads were modeled using models of the traditional polynomial and exponential form, the objective being to demonstrate the effect of present uncertainties in the parameters for such models. UTA, in the RP849-3 project, was to later determine the most appropriate model structures.

The system studies demonstrate the significant effect which load characteristics have on power system stability. Active power characteristics are shown to be most significant, and the nature of the effect of load characteristics on system stability is shown to be dependent on the network configuration, that is, the relationship of the major load and generation areas to one another. One study demonstrated the importance of load model representation relative to excitation system performance, an item generally carefully studied and represented in system stability studies and one representing an investment of up to one million dollars. Although transient stability was the major concern, some consideration was also given to dynamic stability.

Special attention was given to the effect of induction motor load and its dynamics because of the significant portion of the total load made up of this component. Studies were made with the same 2-generator system with induction motor load modeled at a load bus. These results demonstrated that the induction motor load can cause significantly less stable results than for the constant current load model, generally felt to incorporate a significant portion of induction motor load. Some detailed results of these simulations have been documented to indicate the effect of motor load on overall system performance. Motors ranging in size from 10 hp to 5500 hp were considered in the studies. The effects of various modeling assumptions for induction motor characteristics are shown, and the importance of data on motor size, initial loading and shaft load characteristics is demonstrated. Curves showing the steady-state voltage and frequency characteristics are provided for reference purposes.

LOAD COMPOSITION DATA ANALYSIS

Fundamental to the load modeling philosophy being attempted in this project is the need for data to synthesize the composition, by component, of the load bus of

interest. The review of load data sources available to the typical US utility resulted in contacts with nearly all of the components (marketing, planning, economic research, etc.) of a present-day utility.

The data analysis has demonstrated that the load composition of a system bus can be synthesized using data sources which define the devices connected to the bus (load inventory data) and data sources which define the portion of those connected loads which are on at the time of interest (load utilization data). Sources of load inventory data are utility appliance saturation surveys, US census data, component sales data, and utility billing data. Sources of load utilization data are largely made up of load research studies conducted by the electric utilities. These studies make use of demand recorders on sample sets of devices or loads to record the demand at regular intervals (typically 30 minutes) over some period of time (typically 1 year).

Although the data sources in the commercial and industrial sectors are not as prevalent as in the residential sector, the classification by the government and utilities of establishments by Standard Industrial Classification (SIC) is tending to make this data more available as are recent government regulations which require the collection of this data. Also, many commercial and industrial establishments are metered for demand as well as energy.

The methodology of determining load composition using the data sources has been applied to four different utility substations, and an example calculation for one substation is provided. Although problems do exist in obtaining the desired data at all substations, the component method should provide utilities with a significantly more accurate load modeling procedure than exists today.

LOAD MODEL EVALUATION

The UTA load modeling procedure has been evaluated using results from extensive tests at four different substations. Two test sites were used on the Long Island Lighting Company system, and one test site was used on the Rochester Gas & Electric Company system. The fourth test site was located on the Montana-Dakota Utilities Company System. It should be noted that the UTA load modeling procedure itself does not require field tests. On the contrary, the whole thrust of the RP849 Project is to be able to develop load models from typical utility data sources without resorting to field tests.

The LILCO test sites provided mainly residential, rural load areas while the Rochester Gas & Electric Company test site, which consisted of a major portion of downtown Rochester, provided a mainly commercial load. Thus, different classes of loads were tested. Tests were run at each test site during the summer of 1978, the following winter and at one test site on the Long Island Lighting Company system during the summer of 1979. The series of tests at each test site made possible an evaluation of the ability of the UTA load modeling procedure to 'track' the seasonal changes in load composition. Many tests were run during each of these test series, lasting typically a week at each test site. The load tapchanging (LTC) transformers were used to change voltage over a maximum range of +10%. Significant changes in voltage were also accomplished by switching of capacitor banks. At the Southold, LILCO test site a gas turbine-generator, delivering reactive power only, was tripped off the line to produce the most significant changes in voltage. The Southold test site also provided the unique opportunity to determine the frequency response of loads. This load was isolated on the gas turbine-generator, and frequency was varied over a range from 57 to 63 Hz. Changes in voltage were also made in this isolated condition. Several such isolated tests were run during the three different seasons, providing a bank of frequency response data which is unique.

The fourth test site was provided in conjunction with a staged fault test on the Montana-Dakota Utilities Company system in November of 1978. A portion of the Bismarck, North Dakota load was monitored during this fault test, during which voltage reached a low of approximately 40%. This test provided an excellent opportunity to evaluate the capability of the UTA load modeling procedure to model load dynamics. Steady-state voltage change tests were also made at this test site.

The test data from all tests was recorded on magnetic tape with a real time digital data acquisition system (RTDDAS) developed by the Institut de Recherche de l'Hydro-Quebec (IREQ). The data recorded consists of the three phase voltages and currents sampled at rates of from 60 to 150 samples per cycle. These tapes are available for future research. Data processing programs were developed to calculate active and reactive power from the instantaneous voltages and currents.

The UTA load modeling procedure has been found to accurately model the steadystate active power voltage characteristics. Further, the procedure has been found to correctly 'track' the changes in load composition that occur from the summer to winter seasons. Although there are differences between model and test results at some test sites, the UTA load modeling procedure provides a significant improvement over present load modeling procedures.

The tests indicate that there are significant differences between the model and test results for the steady-state reactive power voltage characteristics. The model consistently predicts a lower nominal value of reactive power, and a lower sensitivity to voltage changes than observed during the tests. The most likely sources of error in the model reactive power voltage characteristics are shown to be the component models used for induction motors, fluorescent lights, and distribution transformers. Future research in the load component area would improve the modeling of the reactive power voltage characteristics.

Although there are significant differences on a percentage basis between the model and test results for the active power frequency response, both agree that active power is quite insensitive to frequency changes for the Southold substation. There are significant differences, however, between the model and test reactive power frequency responses. In several cases, the model and test results gave changes in reactive power in opposite directions. The tests also indicated a greater sensitivity of reactive power to frequency changes at high voltages and low frequencies; the model structure is unable to match this characteristic. It may be attributable to saturation of distribution transformers. Again, future research is required.

Identification of load dynamics was aided by the use of the load admittance characteristics in preference to the active and reactive power characteristics. Load admittance allows a separation of the static and dynamic components of load and removes the compounding effect of system voltage changes during transients. As predicted by the model, the dynamic load responses were approximately exponential. However, the active and reactive power responses had different time constants, both of which were significantly greater (2 to 10 times greater) than the single time constant predicted by the UTA load modeling procedure. The UTA model does not adequately model load dynamics.

The recommended research on components should improve the capability of the UTA procedure to model the reactive power voltage and frequency characteristics. A different approach will likely be necessary to model load dynamics.

Section 1 INTRODUCTION

Analysis was done to develop guidelines for use by the University of Texas at Arlington (UTA) in their development of a load modeling procedure. The guidelines were needed to help define the importance of various load model parameters, and the accuracy to which they must be determined. Obviously, effort should not go into modeling load phenomena which have little effect on power system stability. For this reason, emphasis was placed on determining the effects of load models on power system stability. A second use of the system study results was to be in planning the model evaluation portion of the project. The premise was that the evaluation should not be based on simply the differences between model and test parameters but rather on the effect of such differences on power system stability. This research was reported in a task report in July of 1977.

As the total RP849 project evolved, this research on guidelines was not used in either of the above areas. The results are documented here as they help put the load modeling research in perspective and should have considerable reference value. Section 2 summarizes the guidelines.

The initial portion of this research addressed present load model structures which do not include dynamic effects, and the effect of uncertainty in their parameters on power system stability. The results are presented in Section 3 of this report.

Particular emphasis was placed on induction motor loads for two reasons: (1) this component can be the most significant portion of the total system demand (approximately 64% of the electric energy is consumed by electric motors); (2) this component is responsible for most of the dynamics exhibited by the load. Section 4 covers this portion of the research.

Most of the voltage and frequency characteristics of individual components were to be determined in lab measurements by UTA. This approach would be impractical with induction motors because of the wide variety of ratings, inertias, shaft load characteristics, and operating points which exist in practice. For this reason, the effect of such factors were determined for reference purposes with an analytical model. These results are presented in Section 5.

Section 2 SUMMARY OF GUIDELINES

The observations on the work reported in the text are divided into three areas. The first area has to do with general system guidelines and the second area with the effects of induction motor loads in the system studies. The third area deals with induction motor models.

General System Guidelines

- 1. Load characteristics have a significant effect on system stability. Active power models which show a greater change in power for a given change in voltage have the effect of increasing stability for the system configuration where generation is remote to the major load area and decreasing stability for the configuration where generation is local to the major load area. The effect of changing the load characteristics for reactive power is opposite of that for changing the active power representation. Changes in active power load model characteristics are generally more significant in transient stability studies than changes in reactive power load model characteristics. The remote generation configuration showed the greatest sensitivity to load characteristics.
- 2. Polynomial and exponential structured models, equivalent in a dynamic sense at nominal voltage, resulted in nearly identical results for both transient and dynamic stability studies.
- 3. Load representation can be more significant than the generator excitation system characteristics, in its effects on transient stability.
- 4. Load models which represent total power and power factor angle appear to offer some advantages in implementation over representing active and reactive power components.

Induction Motor Dynamics

1. Induction motor load, represented in detail, leads to transient results which do not match those of static load models. The dynamics of the motor have an effect on both transient and dynamic stability.

- Mechanical load inertia is an important factor in system studies as it
 affects both system rotor angle swings and motor stability. It has a
 greater effect than shaft load characteristics of torque versus speed.
 Both effects are dependent on motor size.
- 3. Neglecting rotor and stator electrical dynamics in the induction motor model, which results in a steady-state electrical model coupled with the inertia relations, leads to significantly different results than if the model includes these dynamic effects. This is evident in both system transient response and in the dynamic characteristics of the single induction motor, and is dependent on motor size.
- 4. The steady-state characteristics of active and reactive power as a function of voltage for the induction motor do not adequately represent the behavior during transient operation.
- 5. Dynamic stability analysis of a single motor showed that the characteristics are quite operating-point dependent, and it is difficult to generalize on guidelines.
- 6. To address the question of induction motor aggregation effects, motor loads of two different sizes were applied at a given load bus and the fraction of the bus load supplied by each varied. With 25% of the motor load made up of smaller motors, both size motors (equal inertias were assumed) were prevented from stalling.

Induction Motor Models

- Based on the preliminary studies, saturation in the magnetizing path of the model has a significant effect on the steady-state reactive power at higher than nominal voltage.
- 2. The response of the motor to a disturbance is difficult to characterize in general. Motors with smaller ratings have lower X/R ratios (for standard designs), and first-order effects dominate in the transients. Larger motors are designed with higher X/R ratios and lower slips, and second-order effects are clearly evident in the transient responses.

- 3. The steady-state characteristics of the motor may be useful in load flow or long-term dynamic studies; however, a transient analysis based on these characteristics alone may not be valid.
- 4. Large critical motor loads (5500 HP in this study) or motors with nongeneric design data and shaft load characteristics may have to be modeled in detail for a stability study. The critical size above which a detailed model should be used was not determined.

Section 3 GENERAL SYSTEM GUIDELINES

Existing load model structures, which involved only steady-state, voltage dependent effects, were considered first. The load model structures considered were generally combinations of the traditional constant impedance, constant current, and constant power components. By doing so, no partcular endorsement of any of these was intended. (Recommendations for improved load model structures had to await further RP849 project results.) It was felt that the major difficulty with this and other types of load models was not the model structure but rather uncertainty in the values of the parameters. The emphasis was therefore placed on evaluating the effect of such uncertainty on system studies of transient and dynamic stability.

The inclusion of frequency terms in the load model at the load bus was also studied. For the system disturbances which were used (bolted three-phase faults at a system midpoint bus), frequency excursions were not large, and the effects on the loads were insignificant. Long term dynamic studies involving loss of generation, where significant frequency deviation might be expected, were not performed. These were originally planned, but were cancelled in favor of other EPRI research which was demonstrating the frequency effect.

The two-machine system used for all the studies is shown in Figure 3-1. Two generation areas are indicated at buses 1 and 5, and three load areas at distribution level are shown at buses 6, 7 and 8. The parameters for the line and transformer impedances are given in Appendix A. In all the studies the loads at buses 6 and 7 were both 300 MVA at unity power factor, modeled as constant impedances. For all the general system guideline studies, the third load area had a steady-state load model with a net nominal power of 2400 MVA at 0.9 lagging power factor. The power factor was chosen to give a significant reactive power consumption for consideration of the effect of changes in both active and reactive power load model representation.

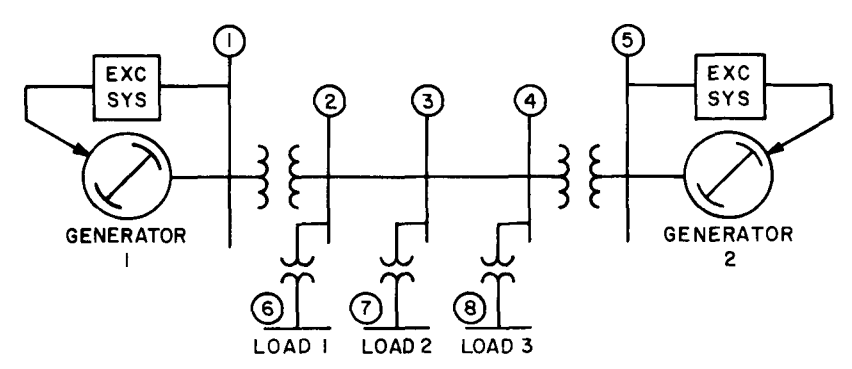


Figure 3-1. Configuration of the two-machine system used in the guideline studies.

The two synchronous machines, each representing some aggregate generation, were sized to consider generation both local and remote to the major load area (bus 8). For the local generation case unit 2 had a 3100 MVA rating and unit 1 a 800 MVA rating. The relative loadings were 2700 MW and 63 MW, respectively. For remote generation the unit ratings were interchanged and the loadings were now 2700 MW for unit 1 and 119 MW for unit 2. Both generators were represented using typical data which is given along with the data on the IEEE Type 1 excitation systems in Appendix A.

The original project plans called for extension of the system guidelines studies to the three-machine, nine-bus WSCC equivalent system using the model developed by UTA. These plans were dropped in favor of having utilities implement the new model structure in full scale stability studies.

TRANSIENT STABILITY

To consider transient stability, a three-phase fault was applied at one point of the two-machine system, and maximum angle swing as a function of fault clearing time was used as the measure of system transient stability. For this two-machine system the maximum angle swing, δ_{MAX} (the maximum rotor angular separation between the two machines), is an indication of how close the machines are to losing synchronism. The fault position for the system with local generation was at bus 3 and with remote generation at bus 7. The reason for changing fault position was to give similar fault clearing times for the same maximum angle swings. The total

fault impedance used in these studies was 0.001 p.u.. The system configuration following fault clearing was assumed to be the same as the pre-fault system configuration. On all of the plotted curves the last stable point is close to the critical clearing time.

Figure 3-2 shows the effect on transient stability of variations in the load model for the active power component of the load at bus 8, with the reactive power representation fixed at constant impedance. The first set of numbered curves (curves 1-3) are for the local generation case, and the second set of curves (curves 4-7) are for the remote generation case. The load models, with the exception of one case for remote generation, were polynomial in form. It should be noted that it was necessary to use a methodology to handle low terminal voltage conditions which existed during fault conditions. A constant impedance formulation was used for static loads in both active and reactive power whenever the voltage at the load was below 0.5 per unit (a continuous function was created). This change was necessary to give a numerically stable solution at lower load voltages, and this approximation is commonly used in large scale transient stability programs.

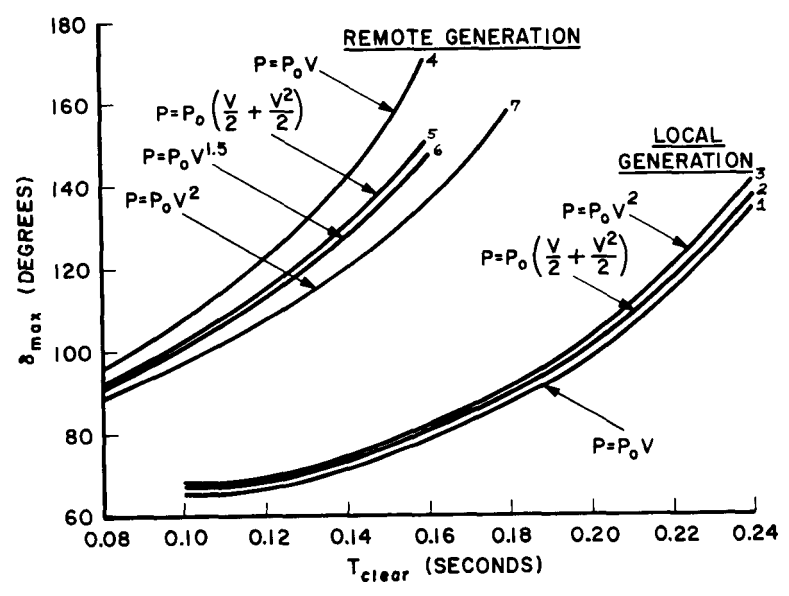


Figure 3-2. Effect on stability of changing active power load models - local and remote generation configurations; reactive power loads modeled as constant impedances.

The results shown in Figure 3-2 indicate that for remote generation, as the load model for active power is changed from constant current (curve 4) to constant impedance (curve 7), the system is more stable for the same disturbance. The effect is significant in the range of 0.15 seconds, which is approximately the time for back-up relaying in an EHV system for remote faults. If primary relaying is assumed, the differences are less significant. It is also interesting to note that there is little noticeable difference in the results as the load is changed from an exponential model with an exponent of 1.5 to a polynomial model, equivalent in a dynamic sense at unity voltage (curves 5 and 6).

The results for the remote generation case can be explained physically as follows: the fault interrupts power transfer from the major generation (bus 1) to the major load area (bus 8); generator 1 will accelerate, and generator 2 will decelerate; a greater reduction of load at bus 8 with the reduction of voltage due to the fault will lessen the deceleration of generator 2 with respect to generator 1 (1-3).

The case of local generation, also plotted in Figure 3-2, shows the opposite effect; increasing the load model exponent in the active power representation leads to less stable results, as expected. The effect of model exponent on stability for the local generation configuration is smaller than for the remote generation configuration.

A corresponding analysis of relative stability for variations in reactive power load model formulation is shown in Figure 3-3. Again the results for the local and remote generation configurations are plotted in this single figure. The active power load model representation is constant current in this study. The resulting effects on transient stability of changing the representation of reactive power are smaller in magnitude and opposite in direction to those of changing the active power representation in both of the generation configurations. The results can be explained physically in terms of voltage support. For example, for the remote generation case, the deceleration of generator 2 is lessened by decreased load at bus 8; loads with more constant reactive power requirements will tend to hold the voltage and load down at bus 8.

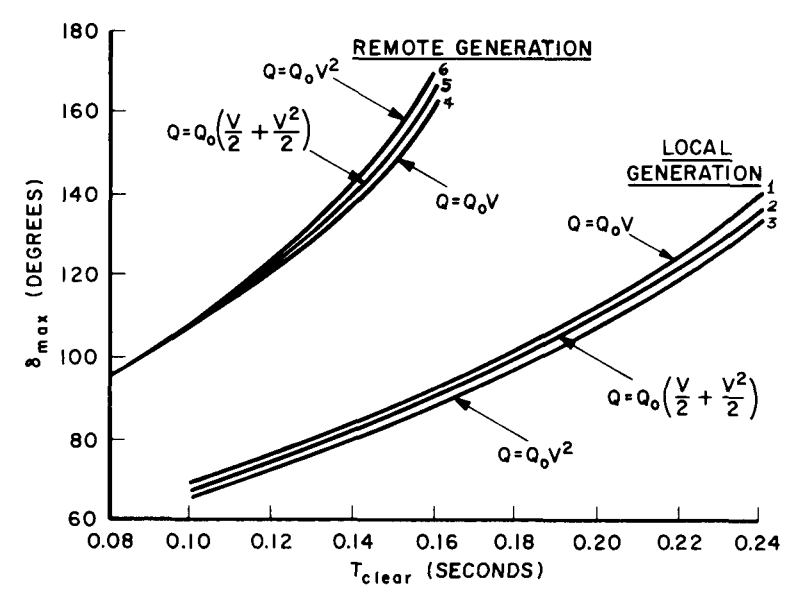


Figure 3-3. Effect on stability of changing reactive power load models - local and remote generation configurations; active power loads modeled as constant currents.

To place the effect of load model representation in perspective, a study was performed to compare the effect of changes in load model with changes in excitation system performance. The previous studies were run with identical high initial response excitation systems (having response ratios of 2.0) on each genera-The results in Figure 3-4 contrast a change in active power load model representation with a change to a low response, conventional excitation system on the larger generator. This study was performed using the system with generation remote from the major load area. Curves 1 and 2 in this figure are duplicates of curves 4 and 7 respectively, in Figure 3-2, showing the effect on stability of changing the active power load model from constant current to constant impedance, respectively. The effect of changing the excitation system on the large remote generator to a 0.5 response conventional exciter (parameters are given in Appendix A) is shown in curve 3 in this figure. The load model representation is constant impedance which corresponds to curve 2. For this particular case the results indicate that load model representation is more significant than changes in excitation systems.

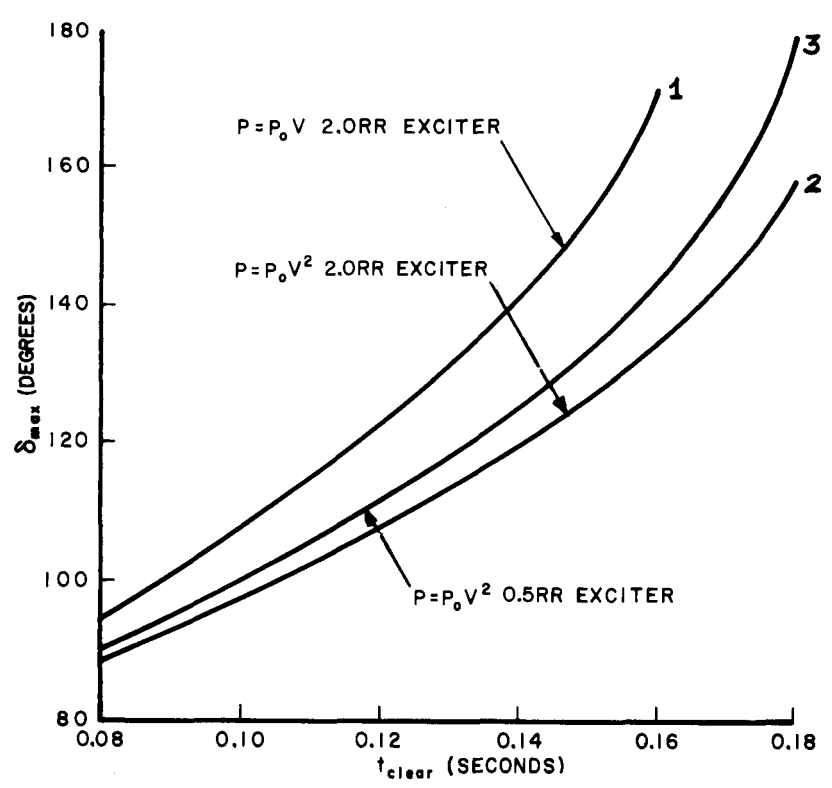


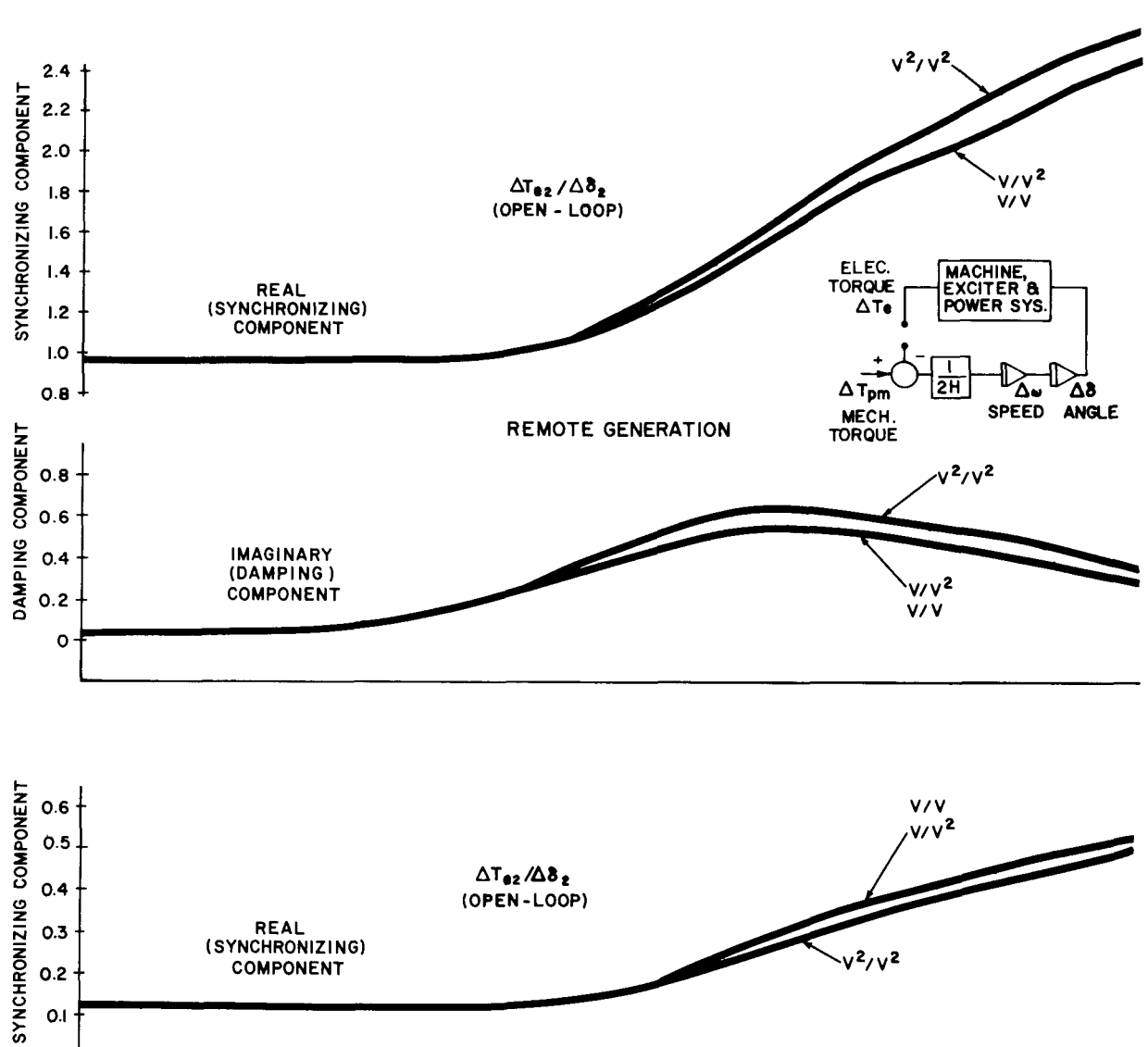
Figure 3-4. Effect on transient stability of excitation system changes relative to changes in the active power load representation.

A final point regarding steady-state load model representation concerns the structure of the model itself. It appears that a model which represents the load in terms of total power and power factor angle might offer significant advantages over a model formulated in terms of active and reactive power components. For polynomial load models the steady-state values are multiplicative terms (for example, $Q = Q_0 F(v,f)$) in the load representation. A formulation in terms of P and Q leads to difficulty in expressing changes in reactive power for unity power factor composite loads (where $Q_0 = 0$).

DYNAMIC STABILITY

The effect of load models on dynamic stability was investigated by plotting the real and imaginary parts of the open-loop transfer function of a change in generator electrical torque for a change in rotor angle. The real part of this transfer function gives a measure of the synchronizing torque component and the imaginary part the damping torque component (4-5). The method of generating the open-

loop transfer function is indicated on Figure 3-5 which shows the small signal performance as a function of perturbation frequency for the remote and local generation cases. (The designation V/V^2 indicates that active power is modeled as a constant current load, or proportional to voltage, V, and that reactive power is modeled as a constant impedance load, or proportional to voltage squared, V^2 .) The plots were made for the machine closest to the load which in the remote generation case is the small machine and for the local generation case is the larger of the two generators. The percentage changes in synchronizing and damping torques are not large, of the order of 10% in the range of 0.5-2 Hz where local mode frequencies usually lie. For the remote generation case, changing from constant impedance to constant current load has a slight de-stabilizing effect whereas for the case of local generation, there is a stabilizing influence for the same change in load model.



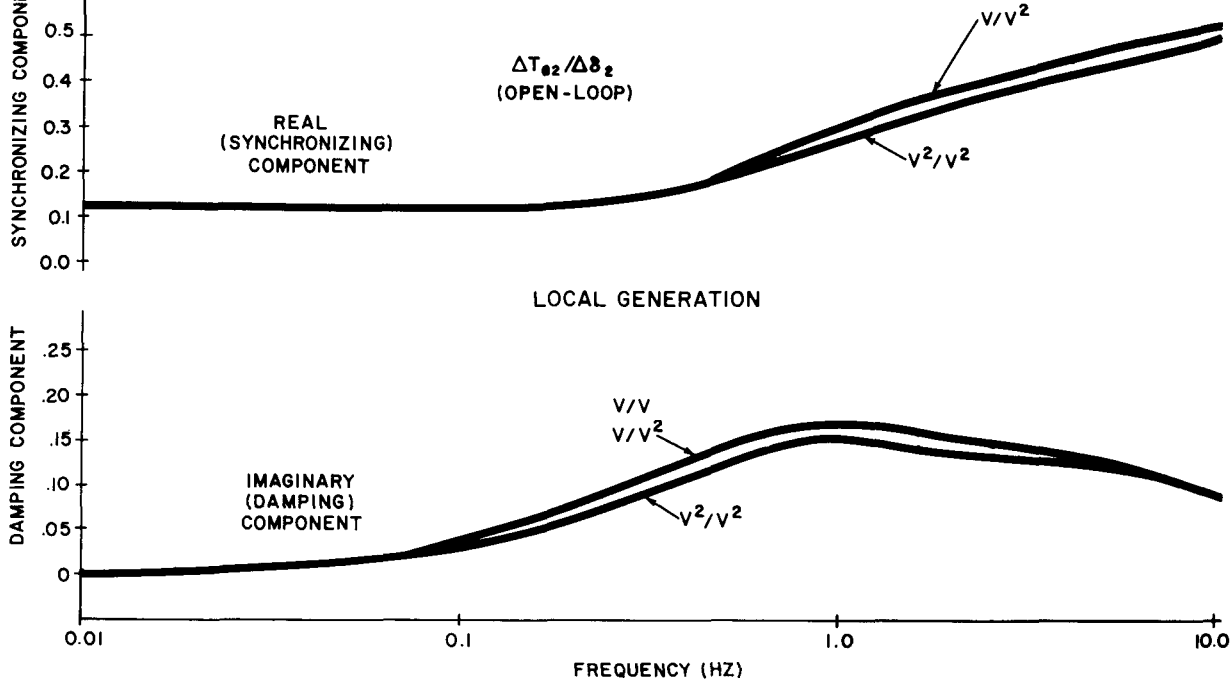


Figure 3-5. Indication of system dynamic stability in the two-machine system as a function of steady-state load model representation; open-loop transfer function of a change in generator electrical torque for a change in rotor angle for generator 2.

Section 4 INDUCTION MOTOR EFFECTS

To determine the effect of dynamic loads on the stability of the system, an induction motor model was added to LOAD 3 shown in Figure 3-1. The model used to represent the motor was a direct and quadrature axis representation with stator electrical dynamics neglected. The resulting model was of third order including the rotor electrical dynamics and mechanical load inertia. The composite motor load was rated at 600 MVA, and the total load at the bus was fixed at 2400 MVA, 0.9 power factor lagging. Thus the load composition at the bus was 25% motor load and 75% static load represented by a polynomial model. The distribution of load as indicated from the power flow gave a motor load of 448 MW and 227 MVAR and a static load of 1712 MW and 820 MVAR. This reflects the fact that the motor mechanical load was only 75% of rated value.

Two motor types were used in these studies, an aggregated motor load which consisted of 30 horsepower motors and an aggregate motor load which consisted of 5500 horsepower motors. The data for each motor type is given in Appendix A. These motors are typical in design and represent sizes near both ends of the spectrum of three-phase motor load. Initial work with the motor model pointed out the need for including saturation of the stator yoke as it effects performance near rated conditions. Saturation data based on design information is given with the motor data in Appendix A.

TRANSIENT STABILITY

Shown in Figure 4-1 is a comparison of stability using the criteria of maximum angle swing as a function of fault clearing time. This is the same criteria which was used for the two-machine system discussed earlier. The total pre-disturbance power and power factor were equal to the values used earlier for the totally static load so that a direct comparison of stability results could be made. From Figure 4-1 it is apparent that having a composite load which is composed of 5500 HP motors leads to significantly greater angle swings than having a composite of 30 HP motors for the remote generation case. There is little difference, however, in the case of local generation.

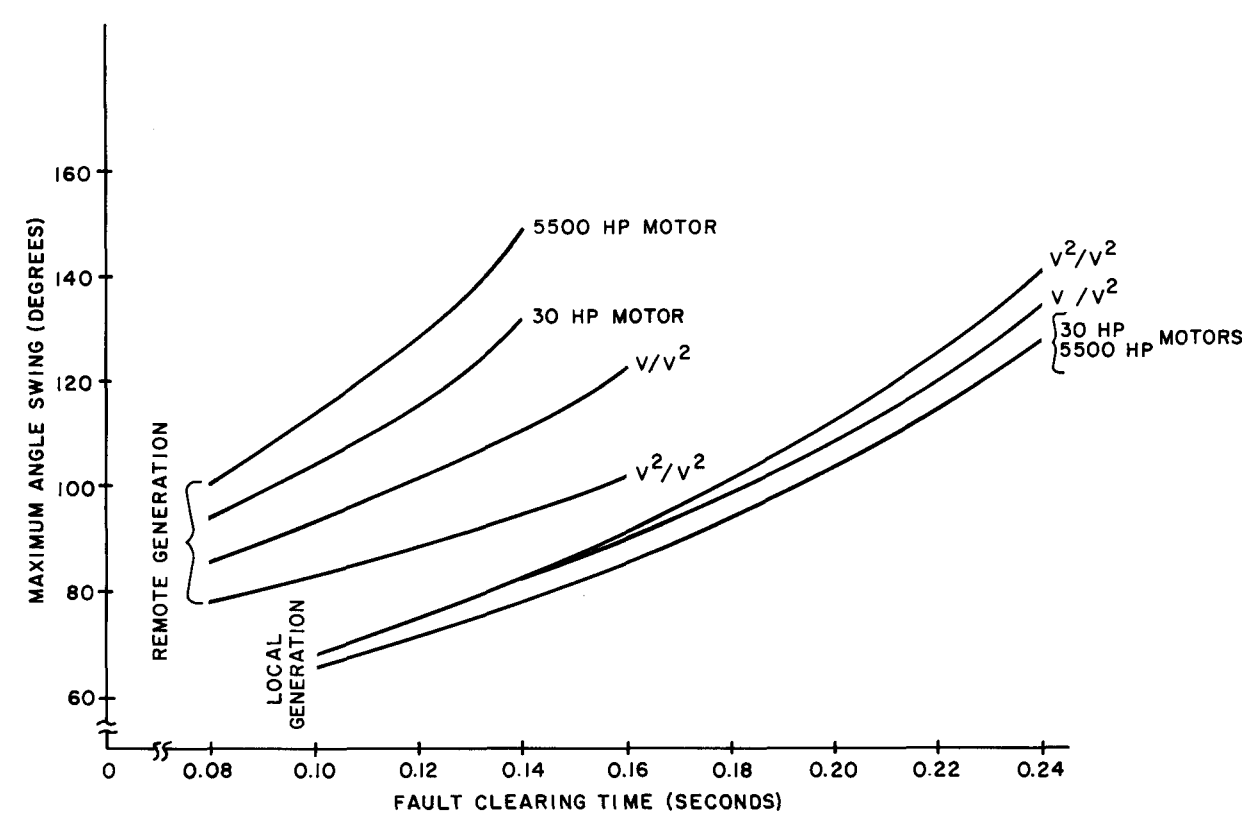


Figure 4-1. Effect on transient stability of modeling induction motor dynamics, relative to use of a totally static load model.

It is worth emphasizing that this motor load is only 25% by rating of the total bus load, the remaining load being constant current for active power and constant impedance for reactive power (denoted in shorthand as V/V^2). The results for totally static load models indicate slightly less stable swings for the local generation case and a substantially more stable swing for the remote generation case. The V/V^2 static load model is an important one because it is sometimes used with the belief that it takes into account the approximately constant active power component of the load caused by induction motors. For the remote generation case such a model would appear to be overly optimistic. The greater the distance, or equivalently the higher the reactance, between the motor load and the major generation area, the more motor dynamics effect transient stability (6-11).

It is of interest to point out that for faults of six cycles or longer, the fraction of load represented as induction motors at the major load area loses stability (monotonic increase in slip) when the 5500 HP characteristic is used. The voltage at the load bus is depressed during the fault, and the significantly greater reactive power demand of the 5500 HP motors as compared to the 30 HP

motors causes the post-fault voltage to be depressed even further. For identical feeder configurations this leads to a case where the motor begins to stall (the same simulation of the motor is used as for normal operation). To further aggravate this situation, a per-unit inertia of H=1.0 was used which is probably unrealistic for a group of motors of 5500 HP rating. Typically these motors would be driving large industrial loads with such loads as ball mills, induced draft fans, and other diversified mechanical loadings. From references in the literature, it appears that combined per-unit inertias in the range of 3-5 are more typical of these drives, and inertias in the 5-10 range are not atypical for some individual motor loads (12,13).

Time response outputs for identical faults with and without a motor load on the system are shown in Figures 4-2 and 4-3. The curves shown in Figure 4-2 are for the case of a 600 MVA motor load composed of 5500 HP motors at the load area and a fault clearing time of 80 milliseconds (about 5 cycles). The variables shown are terminal voltage at generator one, terminal voltage at generator two, active power of the static load, reactive power of the static load, rotor angle difference between the two generators, motor terminal voltage, active power into the motor, reactive power into the motor, and slip of the motor. All variables are in perunit with a base of 600 MVA in the motor variables and 3000 MVA in the system which includes the static load characteristics. In addition, the static load output appears with a negative sign since variables have generator convention. To be compared with Figure 4-2 is Figure 4-3 for the same fault clearing time and system configuration but with an all static load representation of V/V^2 . The same variables are recorded in these two figures, although in a slightly different order, and it is of interest to compare the effect on terminal voltage for the two transient cases. With a fraction of motor load (Figure 4-2) the terminal voltages of both generators are slow in recovering after the fault is cleared, and the voltage at the second generator actually decreases slightly from its post-fault value before it starts to recover. Compare this result with the case of all static load (Figure 4-3) where both generator terminal voltages recover rapidly after the fault is cleared. The reactive power requirement, due to the dynamics of the induction motor, is primarily responsible for the differences in transient responses at the generation areas. It is interesting to note, however, that during the fault, the reactive power to the motor actually changes sign and contributes a stabilizing effect to system voltage profiles.

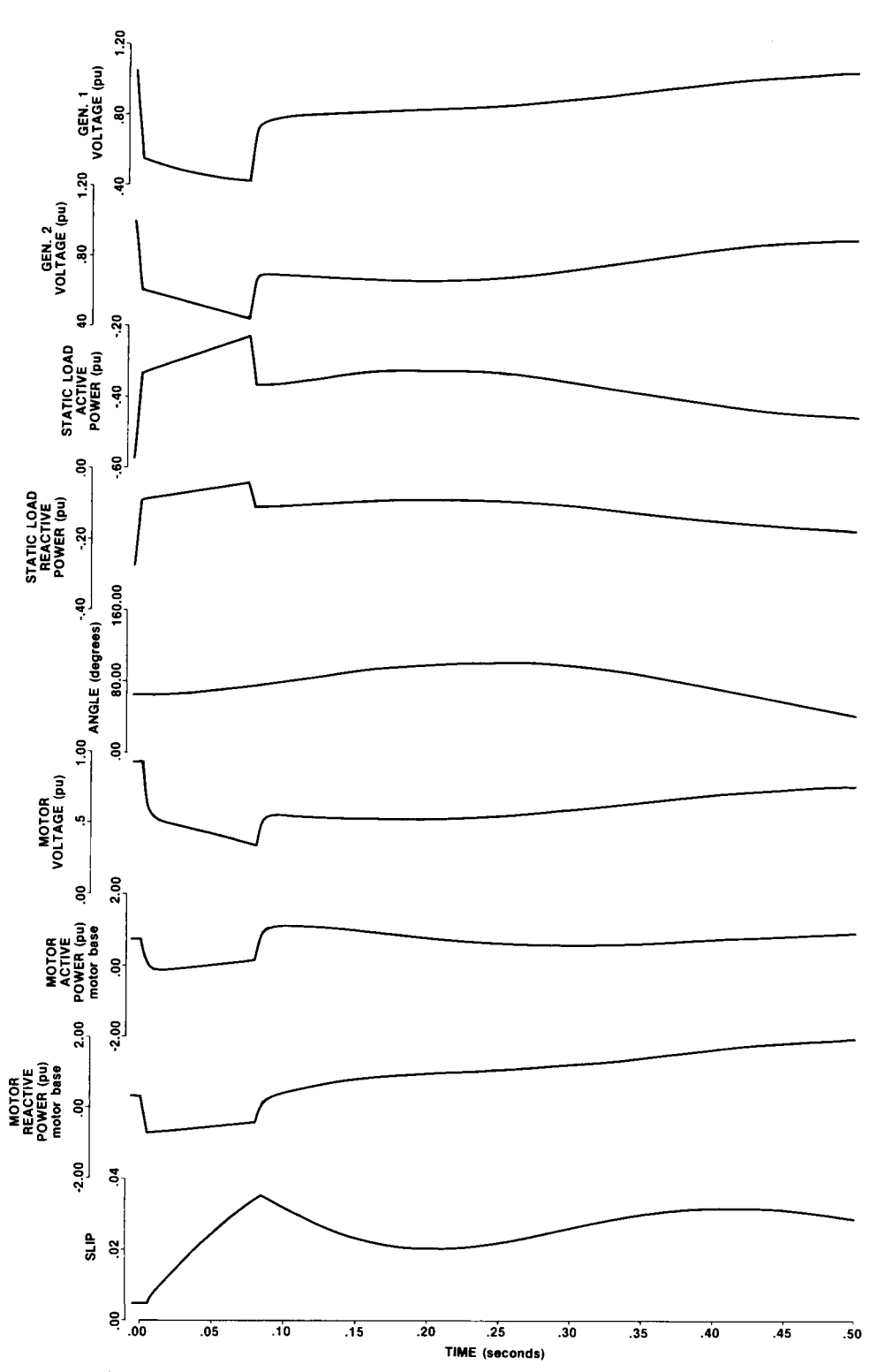


Figure 4-2. Transient response of three-machine system with 5500 hp motor characteristics, remote generation, 80 millisecond fault; motor inertia, H=1.0 sec; shaft torque = 0.75m^2 .

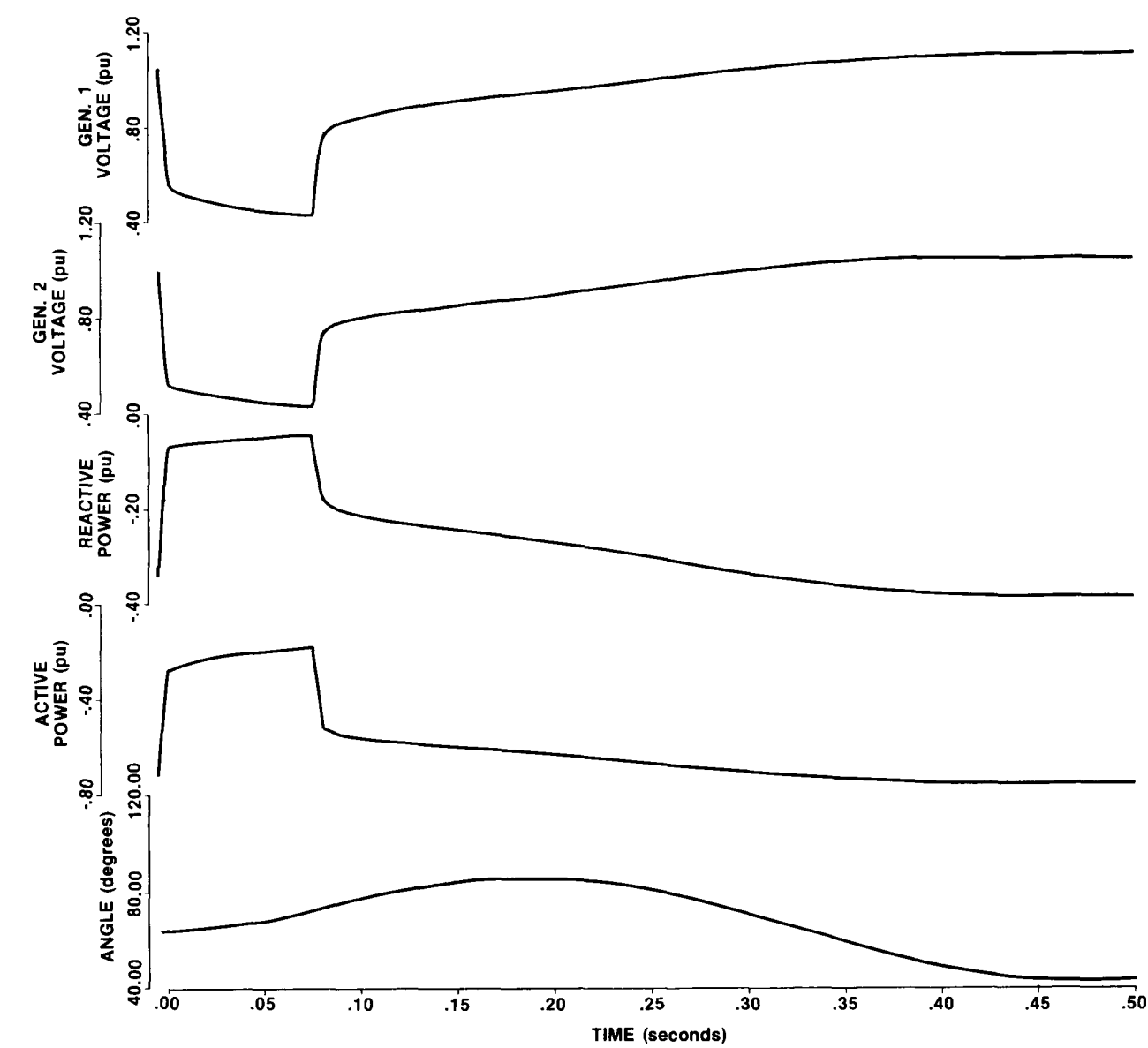


Figure 4-3. Transient response of two-machine system with all static load characteristics (V/V^2) , remote generation, 80 millisecond fault.

The effects on system transients of changing inertias and shaft load characteristics of the motors are shown in Table 4-1. This was done for remote generation and a composite motor load using the 5500 HP characteristics. The first three columns show the effect of varying inertia from H=1.0 to H=5.0 for a shaft load characteristic with torque proportional to the square of rotor speed (typically pump or fan load). The next two columns give results for maintaining the inertia at H=5.0 and changing shaft load to a torque proportional to shaft speed and constant torque, respectively. The last column in Table 4-1 shows the effect on transient performance of a constant shaft torque with the lighter inertia of H=1.0. It is apparent from the results that increased motor inertia has a stabilizing influence on the system. This change also has a stabilizing effect on the motor itself leading to longer fault times before the motor shows signs of instability (stalling). Since the maximum angle swing between the machines is essentially a first swing measure of relative stability, several runs were made for a longer period of time for some of the cases where the motor stalled. It was determined that the motor stalling does not effect the system performance in such a way that instability might occur after the first swing. The induction motor appears as a constant impedance for constant slip operation, and if the motor did indeed reach steady-state at stall, it would appear as a constant impedance load. This question is probably academic in a practical system since contactors or motor protection equipment would take the load out of service for these types of severe, extended transients.

Table 4-1

EFFECT OF VARYING INERTIA AND SHAFT LOAD CHARACTERISTIC FOR 5500 HP MOTOR LOAD
(System Configuration-Remote Generation)

	Maximum Angle Swing (degrees)					
t (seconds)	$T_0 = 0.75\omega^2$ H = 1.0	$T_{\varrho} = 0.75 \omega^2$ $\underline{H = 3.0}$	$T_{\varrho}0.75\omega^{2}$ $H = 5.0$	$T_{q}=0.75w$ $H = 5.0$	$T_{2}=0.75$ $H^{2}=5.0$	$\underline{\underline{\mathbf{H}}}_{\underline{\mathbf{H}}}^{=0.75}$
0.08	100.64	94.41	93.03	93.03	93.04	100.96*
0.10	114.97*	106.49	104.13	104.15	104.16	114.44*
0.12	128.95*	122.60*	118.43	118.46	118.49	128.38*
0.14	149.10*	152.28*	141.74*	141.83*	141.92*	147.71*
0.16						

*motor stalled
--- unstable case

For the transient results presented in Figure 4-1 the motor active and reactive power components were plotted against motor terminal voltage for the 5500 HP motor and remote generation configuration. The results are plotted as solid lines (denoted by P and Q on curves) in Figure 4-4 for a fault time of 100 milliseconds (6 cycles). The motor inertia constant was 1.0 per unit and the shaft load torque was 0.75w^2 . For comparison purposes the steady-state characteristics of the motor for the same shaft load and nominal frequency are shown by the dashed lines plotted in Figure 4-4 (denoted by P_{SS} and Q_{SS} on curves). For the transient response the steady-state operating point is at the far right of the curves, and the direction of movement is in the clockwise direction for advancing time. The jumps or discontinuities in the curves occur when the fault is applied and cleared. These curves are intended to illustrate the differences between the steady-state curves for active and reactive power as a function of voltage and the actual dynamic simulations.

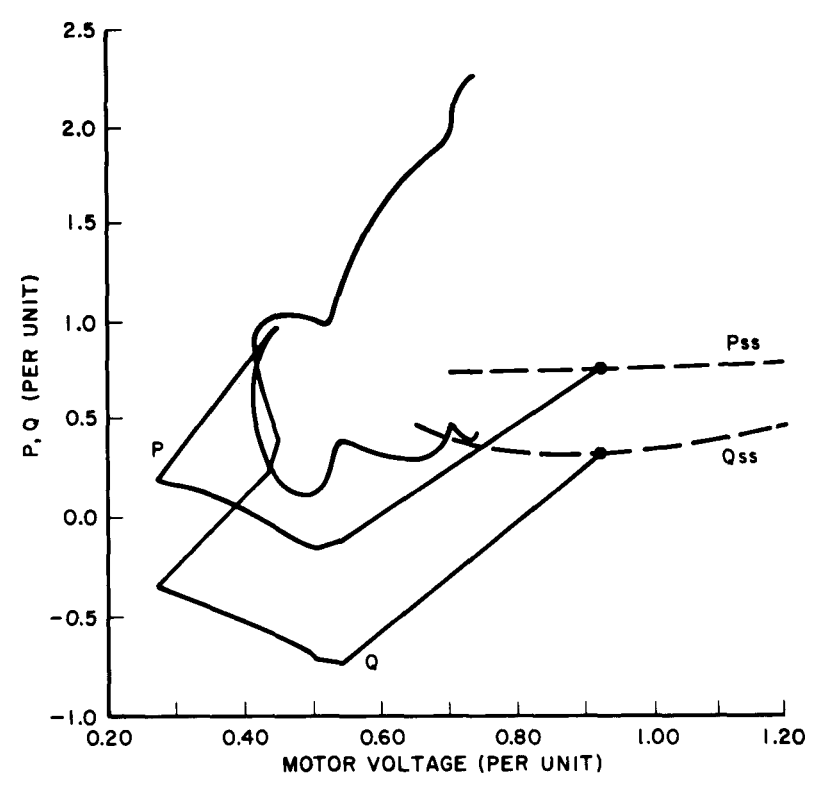


Figure 4-4. Steady-state and dynamic response of 5500 hp induction motor; active and reactive power versus voltage; dynamic response to a 6 cycle system fault.

A simplified representation of induction motor load which has been investigated is the elimination of pw terms in the rotor as well as in the stator electrical circuits. This gives a single state model for the induction motor which has essentially a steady-state electrical model coupled with the inertia effects $(\underline{14,15})$. Table 4-2 shows the results of duplicating previously run transient system studies for the remote generation configuration using the 30 HP and 5500 HP motor characteristics both with and without rotor electrical dynamics. Neglecting rotor pw terms leads to more stable swings, with a greater percentage change for the large motor sizes. Neglecting rotor electrical dynamics also has a secondary effect on motor stability. The optimistic results obtained with the simpler first order model have been previously recognized in the literature $(\underline{15,16})$, and caution should be exercised in using this model in system studies.

Table 4-2

EFFECT OF NEGLECTING ROTOR ELECTRICAL DYNAMICS ON TRANSIENT STABILITY

OF THREE-MACHINE SYSTEM

Remote Generation All Motor H = 1.0, $T_{\ell} = .75 \omega^2$

t _{clear}	30 HP Data with dynamics	Maximum Angle Sw 30 HP Data without dynamics	ing (degrees) 5500 HP Data with dynamics	5500 HP Data without dynamics
0.10	104.38	101.49	114.47*	102.77
0.12	116.55	112.74	128.95*	113.43*
0.14	132.46	126.88	149.10*	126.8 2 *
0.16		149.66*		147.35*

*motor stalled
--- unstable case

For the remote generation configuration, the results in Table 4-3 show the effect of varying the mix of motor type while maintaining the net motor rating at an aggregate of 600 MVA $(\underline{17},\underline{18})$. The system configuration is the same, and two motor models were simulated at the major load bus. Again, the total power was adjusted so that it equalled 2400 MVA at 0.9 power factor to match the steady-state operating point used in the previous studies.

Table 4-3

EFFECTS OF AGGREGATION USING TWO INDUCTION MOTORS ON TRANSIENT STABILITY

Remote Generation All Motors Have H = 1.0, T_{ℓ} = .75 ω^2

t clear seconds	600 MVA 30 HP Motor	Maximum Angle 3 400 MVA-30 HP 200 MVA-5500 HP	Swing (degrees) 200 MVA-30 HP 400 MVA-5500 HP	600 MVA 5500 HP Motor
0.10	104.38	106.79	109.41	114.47*
0.12	116.55	119.93	123.81	128.95*
0.14	132.46	138.18*	146.19*	149.10*
0.16				

*motor stalled
--- unstable case

Results from Table 4-3 show that varying the motor mix leads to an averaging effect. It is interesting to note that with a conversion of only one third of the aggregate motor load to 30 HP motors, several cases where the 5500 HP motors had previously stalled now show stable motor operation. There is only one indication of motor stability given in the table since, for the particular cases which were studied, if one motor type stalled for a given transient, the second motor type also stalled. One phenomena which was noted but not explored in detail was the possibility of transfer of power during a transient between induction motor groups. This effect is predominant when the mechanical load inertias are significantly different (12,13). In the studies reported here, the two induction motor groups were modeled in computer subroutines with the same bus variables as inputs; transfer of power between the groups was not modeled.

DYNAMIC STABILITY

To consider the effects of the induction motor on system dynamic stability, the dynamic stability of a single induction motor was first reviewed, and then a system approach was considered for the three-machine system. A review of the literature shows work done in this area detailed in References 16, and 19-24.

Table 4-4 shows the poles and zeros of the transfer functions ($\Delta P/\Delta V$ and $\Delta Q/\Delta V$) for the 5500 HP induction motor (data listed in Table 5-1) at various initial voltage levels. Figures 4-5 and 4-6 show plots of the gain and phase for the $\Delta P/\Delta V$ and $\Delta Q/\Delta V$ transfer functions, respectively. It is obvious from the results of these studies that the dynamic characteristics of the induction motors vary widely with initial operating points. In fact, as initial voltage changes, some of the transfer functions change from minimum to non-minimum phase expressions ($\underline{16},\underline{19}$). There does not appear to be a simple form that can be postulated that will accurately represent the small signal behavior of the motor over a wide range of operating conditions.

Table 4-4
TRANSFER FUNCTIONS FOR 5500 HP INDUCTION MOTOR

Terminal Voltage	Transfer Function	Steady-State Gain	Zeros	Poles
V _t =0.8 pu	ΔΡ/ΔV ΔQ/ΔV	1.339	+5.231 -8.21+j10.53 +2.389 -6.37+j18.94	-6.165 -5.37+j19.64 -6.165 -5.37+j19.64
V _t =1.0 pu	ΔΡ/ΔV ΔQ/ΔV	1.100 4.826	+.5041 -7.91 <u>+</u> j9.63 -1.510 -4.99 <u>+</u> j25.63	-7.784 -4.57±j26.21 -7.784 -4.57±j26.21
V _t =1.2 pu	ΔΡ/ΔV ΔQ/ΔV	0.9397 5.785	+.5102 -7.57 <u>+</u> j9.86 -1.621 -4.57 <u>+</u> j31.55	-8.186 -4.38+j31.90 -8.186 -4.38+j31.90

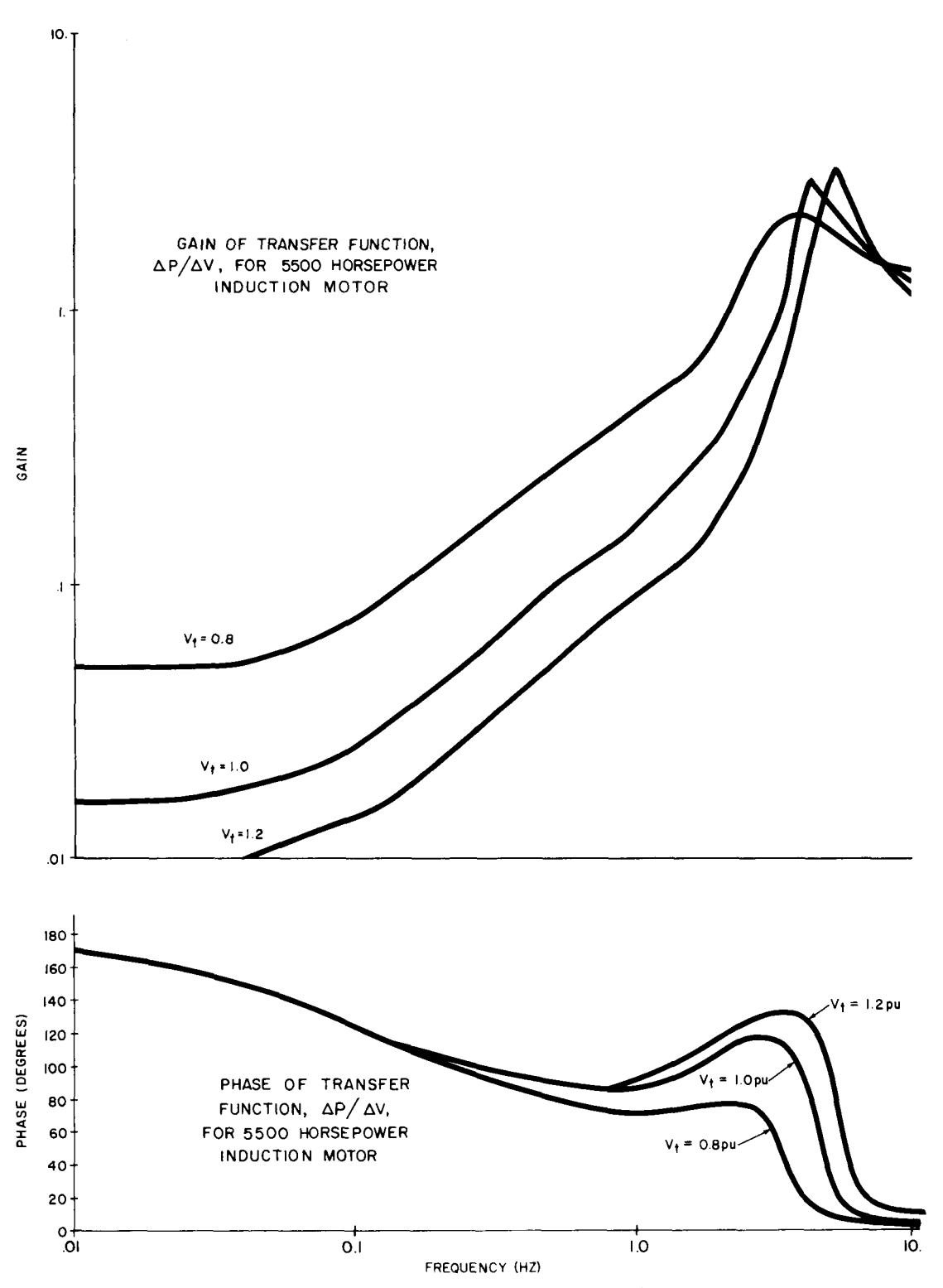


Figure 4-5. Gain and phase of transfer function, $\Delta P/\Delta V,$ for 5500 hp induction motor.

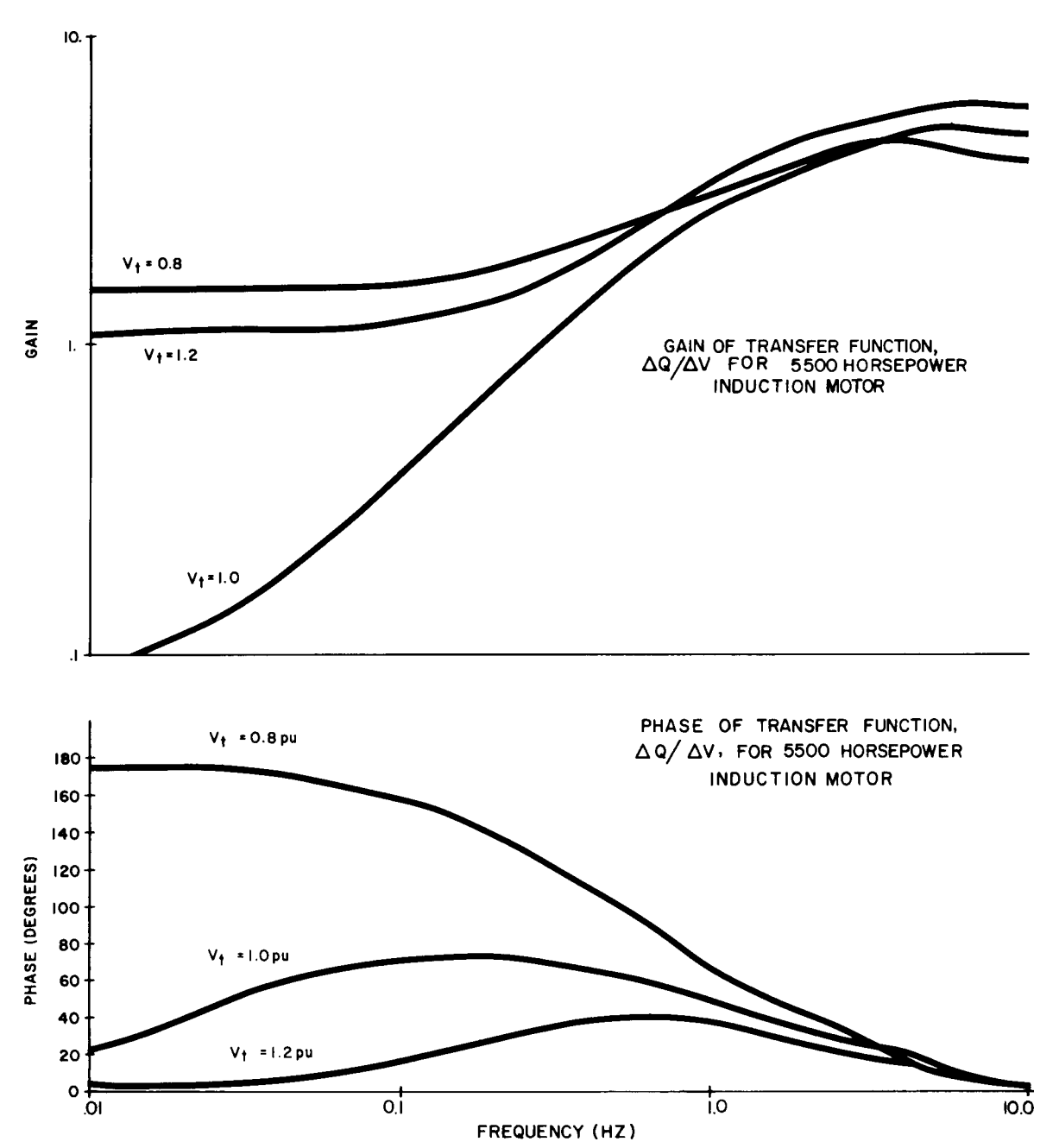


Figure 4-6. Gain and phase of transfer function, $\Delta Q/\Delta V,$ for 5500 hp induction motor.

For the three-machine system, an indication of the effect of the induction motor load on dynamic stability can be seen by looking at the eigenvalue corresponding to the local mode oscillation between the two generators. Table 4-5 shows the results for the case of remote generation, a motor inertia H=1.0, and a load on the motor of $T_{\ell}=0.75\text{m}^2$. The case of all static load is shown first for comparison purposes.

Table 4-5

LOCAL MODE EIGENVALUE FOR TWO-GENERATOR SYSTEM WITH LOAD REPRESENTATION VARIED

Load Representation	Eigenvalue	Damping Ratio
All V/V ² Static Load Motor with Rotor Dynamics	-1.72+j11.16 -1.66+j11.06	153 148
Motor without Rotor Dynamics	-2.17 - j11.61	184

There is a slight decrease in damping, shown by the damping ratio in the last column, with the motor represented in detail as compared to an all static load representation. The motor without dynamics in the rotor electrical circuits causes a significant increase in damping. Both the transient and dynamic performance of this simplified, first order model lead to reservations about its accuracy in system studies.

Section 5

INDUCTION MOTOR PERFORMANCE ANALYSIS

The steady-state and dynamic load characteristics of most of the load components considered in this project were measured in lab and field tests by the University of Texas, Arlington. However, since it would be impractical to test motors of widely different ratings with different load inertias and shaft load characteristics, it was decided that an analytical model would be necessary to determine the load characteristics of induction motors. For this reason, the steady-state and transient load characteristics of a number of induction motors were determined, for use by UTA, using an existing induction motor model.

This analysis work can be divided into the following general study objectives:

- Analysis of the steady-state operation of induction machines over a wide range of supply voltages and frequencies.
- 2) Transient responses of the motors to large disturbances and the effect of motor parameters on characteristic performance.

DESCRIPTION OF THE MODEL

The analytical model used to represent the induction motor has previously appeared in the literature (25-27). A symmetrical three-phase induction motor is represented by voltage equations which have been transformed into the direct and quadrature axes. These equations, when expressed in the synchronously rotating reference frame, lead to the equivalent circuits shown in Figure 5-1.

The method of including saturation in the magnetizing path is described in References $\underline{25}$ and $\underline{26}$. If stator electrical transients due to p Ψ terms are to be neglected, the resulting equations are detailed in Reference $\underline{27}$. For frequencies within a power system up to and including local mode and intertie swing frequencies, the approximation of excluding the stator p Ψ terms is valid ($\underline{27}$ - $\underline{29}$). The model which was used to obtain the transient results for this task does not include p Ψ terms in the stator equations or network equations.

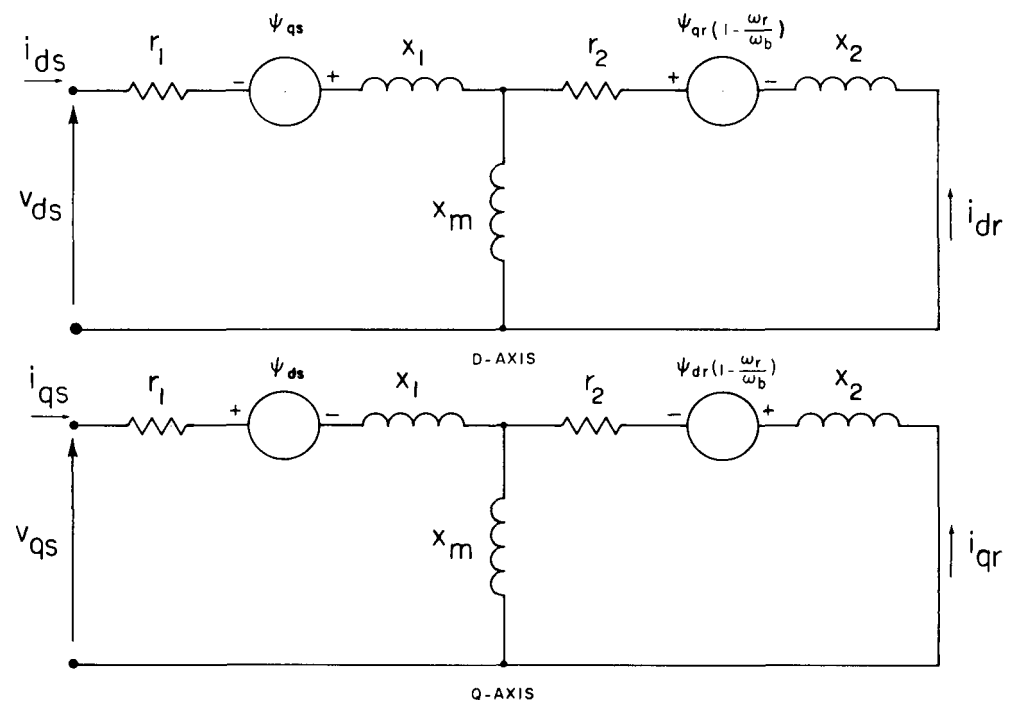


Figure 5-1. Induction motor equivalent circuit in d and q axis representation and synchronously rotating reference frame.

STEADY-STATE RESULTS

For the purposes of conducting this phase of the loads guidelines task, design data for nine machines ranging in size from 10 to 5500 horsepower were made available by two different General Electric departments. A summary of these parameters is shown in Table 5-1. Four motors in sizes of 10, 30, 250 and 5500 horsepower were chosen as representative to develop steady-state operating characteristics. The steady-state operating characteristics were determined for active and reactive power as a function of terminal voltage for various shaft load characteristics, and supply frequency was varied between 57 and 63 Hz (+ 5%). Initially, the effects of saturation in the flux paths of the motors were neglected. Comparison of the resulting curves with those published in the literature (3,15,30-32) and other test results, showed a smaller increase in calculated reactive power required by the motor as terminal voltage was increased from rated to 120% of rated value. Saturation was included in the magnetizing path of the induction motor model to account for this effect. The data for the saturation curves, which is shown in Figure 5-2 for these four motors, was derived from the outputs of motor design programs. Inasmuch as saturation is not normally included in motor design specifications, these curves have not been verified by test at any point other than rated voltage. Saturation in the rotor slot wedges was not represented due

Table 5-1 INDUCTION MOTOR DATA*

	Voltage &	2-l						Base		
<u>HP</u>	(Volts)	<u>kVA</u>	<u>XM**</u>	<u>X1</u>	<u>X2</u>	<u>R1</u>	<u>R2</u>	Ohms	RPM	H(sec)
10	460	7.46	1.69	.071	.105	.044	.021	28.37	1800	.076
30	460	22.38	2.92	.086	.149	.025	.0153	9.46	1800	.124
100	460	74.60	2.75	.062	.163	.0153	.0088	8.51	1800	.256
250	460	223.97	4.15	.154	.089	.0267	.0145	2.83	1800	.201
300	460	223.80	3.00	.070	.126	.0141	.0099	2.84	1800	. 206
800	2300	707.5	3.20	.120	.072	.0122	.0100	2.48	1200	. 245
3000	4160	2556.5	6.06	.171	.083	.0098	.0089	6.77	1800	.350
4000	4160	3362.8	4.83	.166	.047	.0046	.0058	5.15	3600	.903
5500	4000	4793.6	3.75	.127	.110	.0057	.0052	3.34	900	.483

 \dot{x} All resistance and reactance values are given in per-unit on the given impedance base.

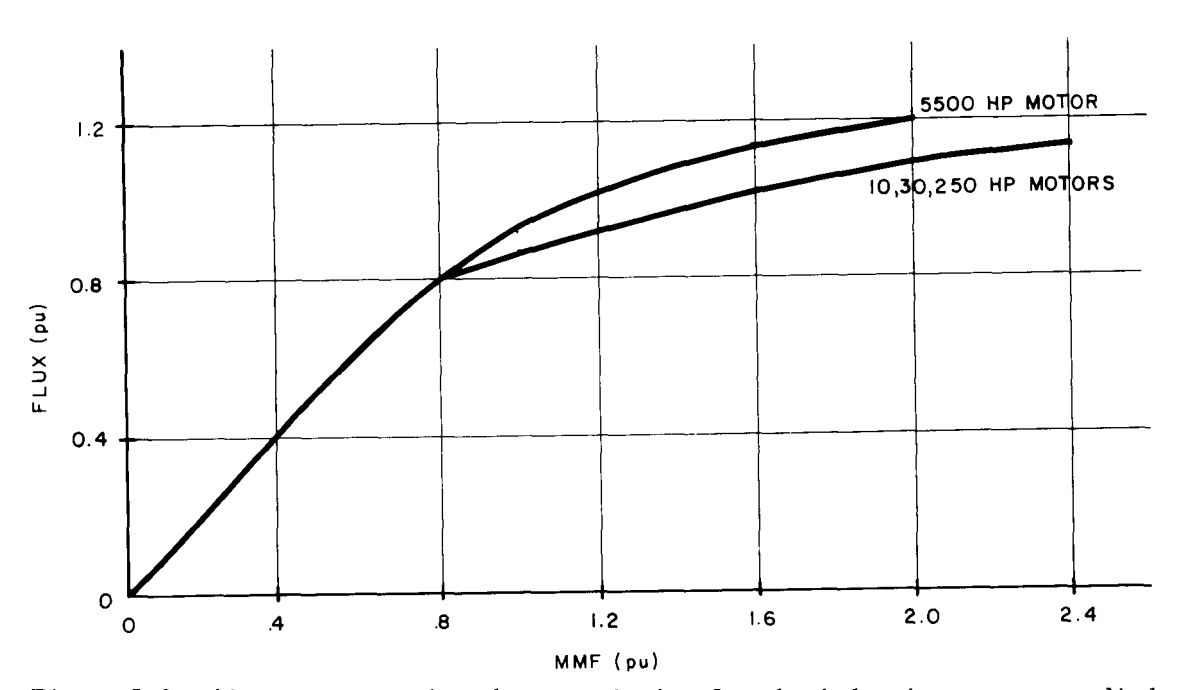


Figure 5-2. Air-gap saturation characteristics for the induction motors studied.

to the fact that this effect only becomes significant at high rotor current levels under such conditions as motor starting, which was not within the scope of this project.

The curves for steady-state motor power as a function of terminal voltage were plotted using a scale for active and reactive power which is normalized to the operating point at rated terminal voltage. This enables a convenient base of comparison for changes in shaft load torque and load characteristics as well as system frequency. In order to convert the normalized values to per unit watts and vars, the data in Table 5-2 shows the steady-state per unit operating points at rated terminal voltage.

Table 5-2
INDUCTION MOTOR STEADY-STATE OPERATING POINTS

At rated terminal voltage including the saturation effects of the magnetizing reactance

Per Unit P(Q) for Shaft Load Torques of -							
HP	Freq.	0.75	0.75ω ²	1.0	1.0w ²	1.25	<u>1.25ພ²</u>
10	57 Hz 60 Hz 63 Hz	.79(.56)	.76(.55)	1.01(.67) 1.07(.63) 1.12(.62)	.97(.66) 1.01(.61) 1.06(.59)	1.35(.74)	1.26(.70)
30	57 Hz 60 Hz 63 Hz	.77(.43)	.75(.42)	.98(.55) 1.03(.54) 1.09(.56)	.95(.54) 1.00(.53) 1.05(.53)	1.30(.71)	1.24(.67)
250	57 Hz 60 Hz 63 Hz	.77(.33)	.75(.34)	.98(.46) 1.03(.47) 1.09(.50)	.95(.44) 1.00(.45) 1.05(.47)	1.31(.65)	1.25(.61)
5500	57 Hz 60 Hz 63 Hz	.75(.39)	.75(.39)	.96(.49) 1.01(.51) 1.06(.54)	.95(.49) 1.00(.50) 1.04(.53)	1.26(.68)	1.24(.65)

Representative results are included here for two of the motors analyzed. Figures 5-3 through 5-6 show data for the 30 horsepower motor, followed by a similar set of curves for the 5500 horsepower motor (Figures 5-7 through 5-10). Figure 5-3 shows the reactive and active power for constant load torques of 125%, 100%, and 75% of rated as a function of supply voltage. Figure 5-4 shows the reactive and active power for ± 5% frequency changes with various supply voltages for a constant rated load torque. Figures 5-5 and 5-6 are the same as the first set with the exception that the load torque was proportional to the square of rotor speed. All computer runs were made for supply voltages of 0.5 to 1.2 per unit. Where points are not plotted on the graphs at lower voltage levels, the motor would not support the given load torque in steady-state operation.

With a constant shaft load torque (for example, an elevator), the active power tends to increase slightly as voltage is decreased. This change decreases as motor size increases. With a shaft load torque proportional to the square of motor speed, which is more representative of pump or fan load characteristics, the changes in active power move in the same direction as changes in terminal voltage. The changes are quite small in both cases, and for all practical purposes the active power can be considered to be constant in steady-state operation. Reactive power drawn by the motor as a function of terminal voltage shows a more significant effect. Significant increases in reactive power occur for both high and low voltages. The smaller motors show a greater increase in reactive power at high voltages due to the lower number of poles and the structure of the stator yoke. The larger motors which have higher X/R ratios show a greater increase in reactive power at lower terminal voltage. The increase in reactive power which occurs at low voltages is a significant phenomenon in that it works to prevent motor recovery following a system fault; voltage tends to be depressed for longer periods of time.

The curves showing the effect of supply frequency changes on steady-state operating point (Figures 5-4, 5-6, 5-8, 5-10) are also plotted with terminal voltage as an independent variable. Frequency effects are shown as parametric changes in the plotted curves. As might be expected, frequency appears to have little effect on active power and is most noticeable in reactive power characteristics. The effect of frequency on the operating point is comparable to changing shaft load characteristics and is a secondary effect to terminal voltage changes, at least in the range of interest specified in this project.

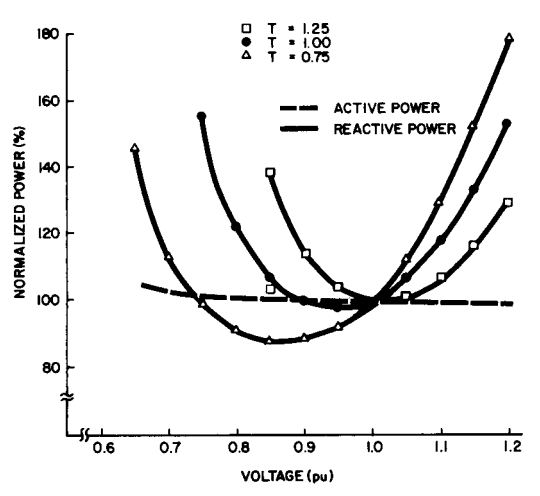


Figure 5-3. Motor input power versus voltage for 30 hp motor, constant shaft torque.

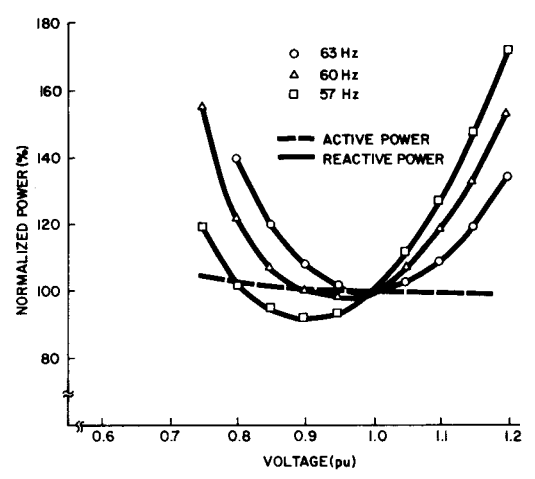


Figure 5-4. Motor input power versus voltage for 30 hp motor, rated torque, +5% frequency variation.

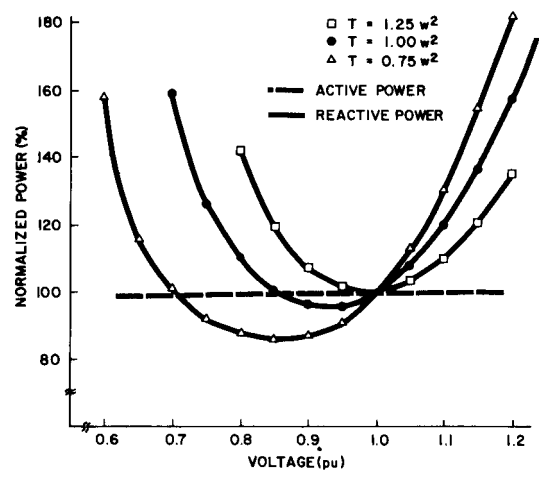


Figure 5-5. Motor input power versus voltage for 30 ${\rm hp}_2{\rm motor}$, shaft torque proportional to ${\rm w}^2$.

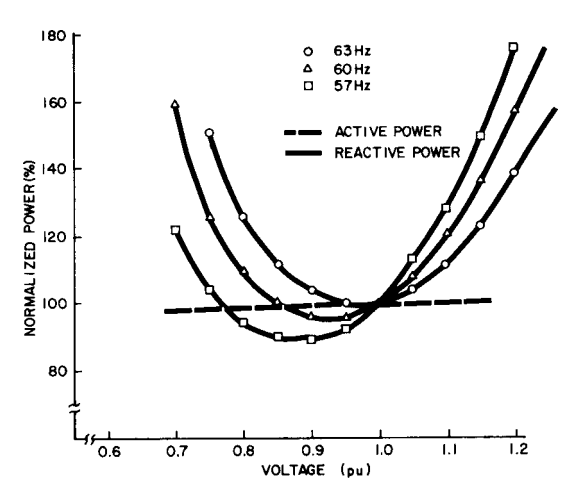


Figure 5-6. Motor input power versus voltage for 30 hp₂motor, rated torque proportional to w^2 , $\pm 5\%$ frequency variation.

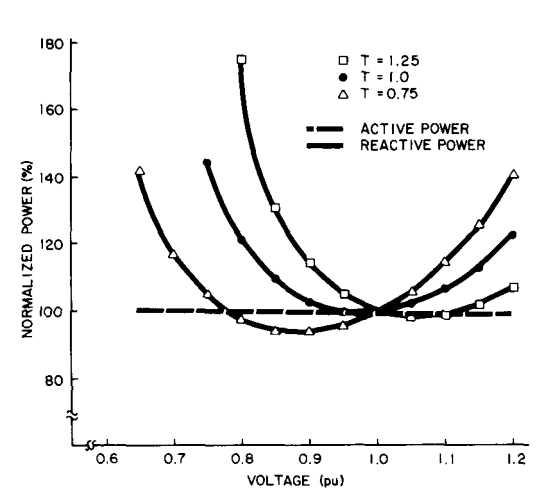


Figure 5-7. Motor input power versus voltage for 5500 hp motor, constant shaft torque.

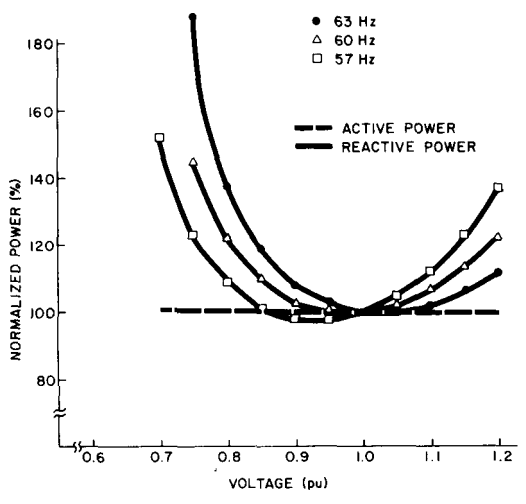


Figure 5-8. Motor input power versus voltage for 5500 hp motor, rated torque, +5% frequency variation.

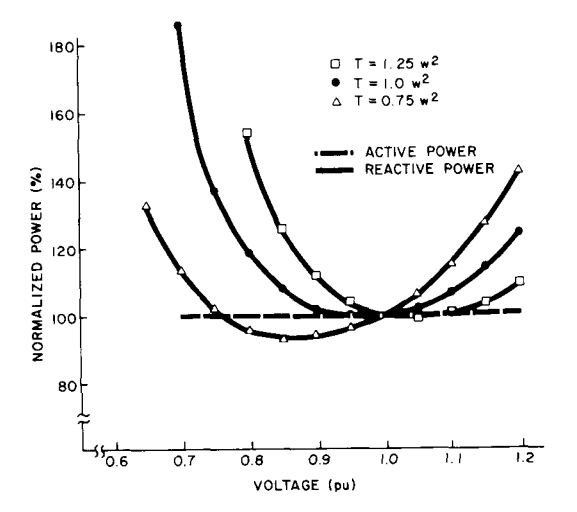


Figure 5-9. Motor input power versus voltage for 5500 hp motor, shaft torque proportional to ω^2 .

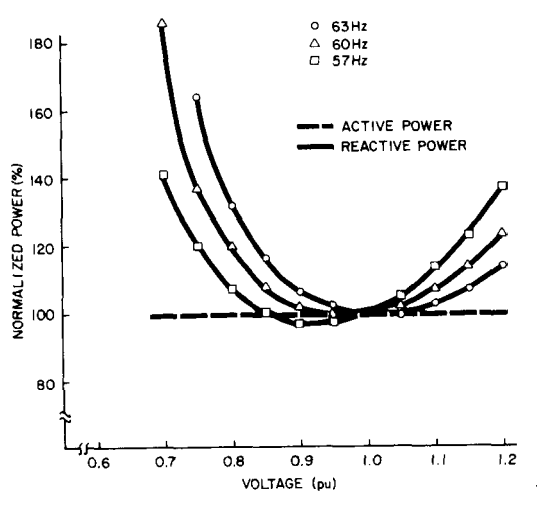


Figure 5-10. Motor input power versus voltage for 5500 hp motor, rated torque proportional to ω^2 , $\pm 5\%$ frequency variation.

TRANSIENT RESULTS

Computer simulations of representative transients were run using the data corresponding to the 30 HP and 5500 HP motors. Each motor was simulated as being connected to a stiff system through a transformer and line impedance as shown in Figure 5-11.

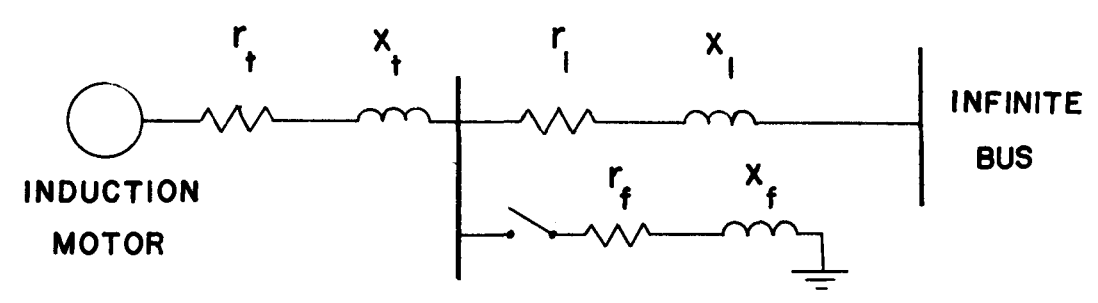


Figure 5-11. System for study of single induction motor transients.

A high impedance three phase fault was applied at the high side of the transformer to simulate the voltage profile which might occur in an actual feeder due to a fault within the remainder of the system. The impedance values were as follows: transformer impedance, $\mathbf{r}_t = 0.01$, $\mathbf{x}_t = 0.10$; fault impedance, $\mathbf{r}_f = 0.20$, $\mathbf{x}_f = 0.40$; line impedance, $\mathbf{r}_1 = 0.01$, $\mathbf{x}_1 = 0.10$. These impedances are in per unit on the base corresponding to the motor rating. The fault time was 100 milliseconds (six cycles). The machines were loaded with rated torque which was proportional to the square of rotor speed. Saturation was included in the magnetizing path. The per-unit inertias which were used to represent the combination of rotor and load inertia were 0.75 sec for the 30 HP machine and 1.0 sec for the 5500 HP machine. A higher inertia was used for the 5500 HP machine due to the rotor itself having a higher inertia constant (refer to Table 5-1).

Figures 5-12 and 5-13 show motor variables which are as follows: Slip-change in rotor speed from base speed, $Q_{\rm T}$ - reactive power at the terminals of the motor, $P_{\rm T}$ - active power at the terminals of the motor, $I_{\rm term}$ - magnitude of terminal current and $E_{\rm term}$ -magnitude of terminal voltage. These variables are all in per unit on the motor rating base, and power is expressed as positive when absorbed by the motor. For the 30 HP motor (Figure 5-12), the motor terminal voltage decays to approximately 82% before the fault clears, whereupon there is what appears to be a simple first order response as the motor returns to the original operating point when the fault clears. With the same disturbance applied to the 5500 HP

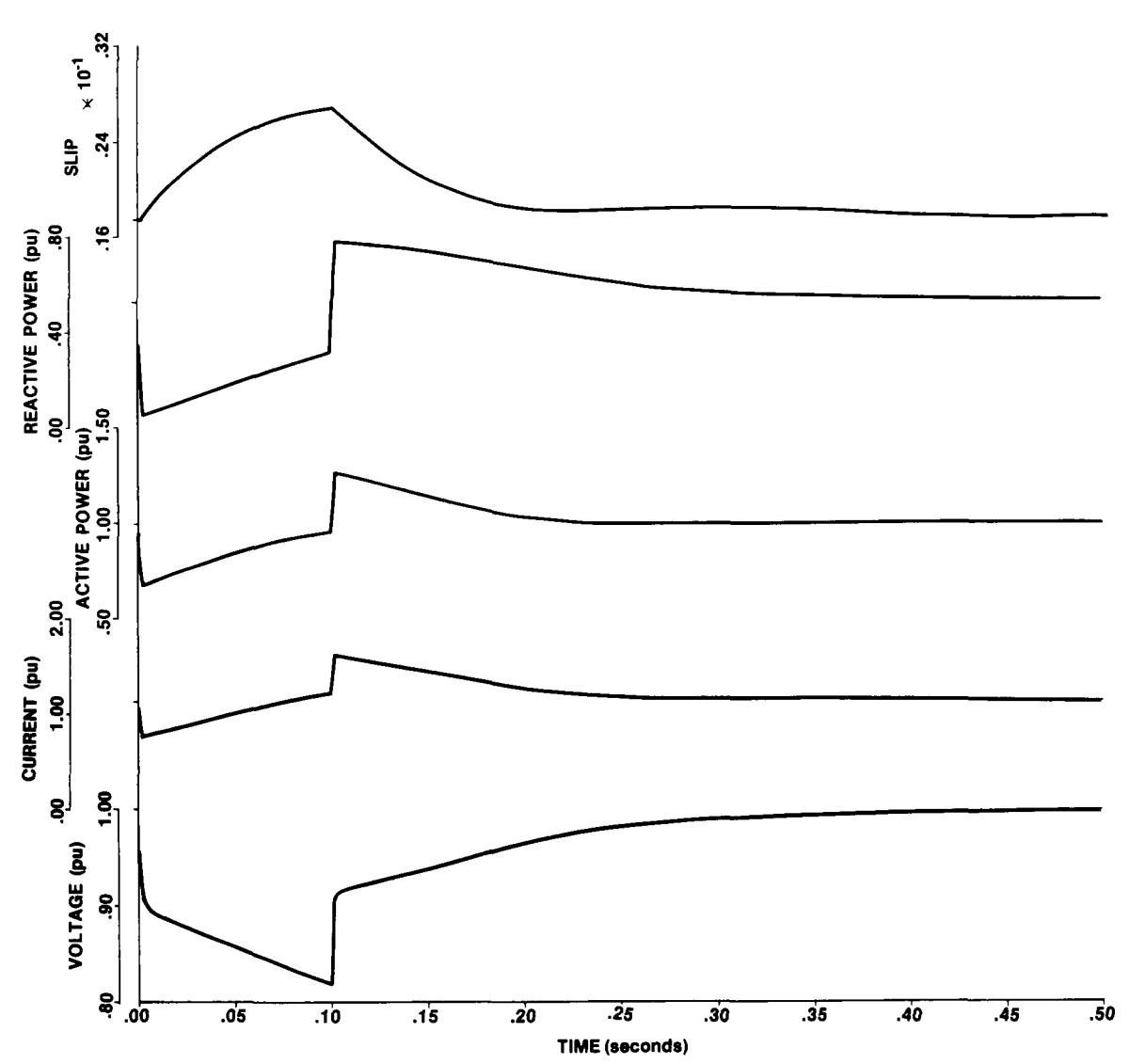


Figure 5-12. Transient response for 30 hp motor; single motor to infinite bus system.

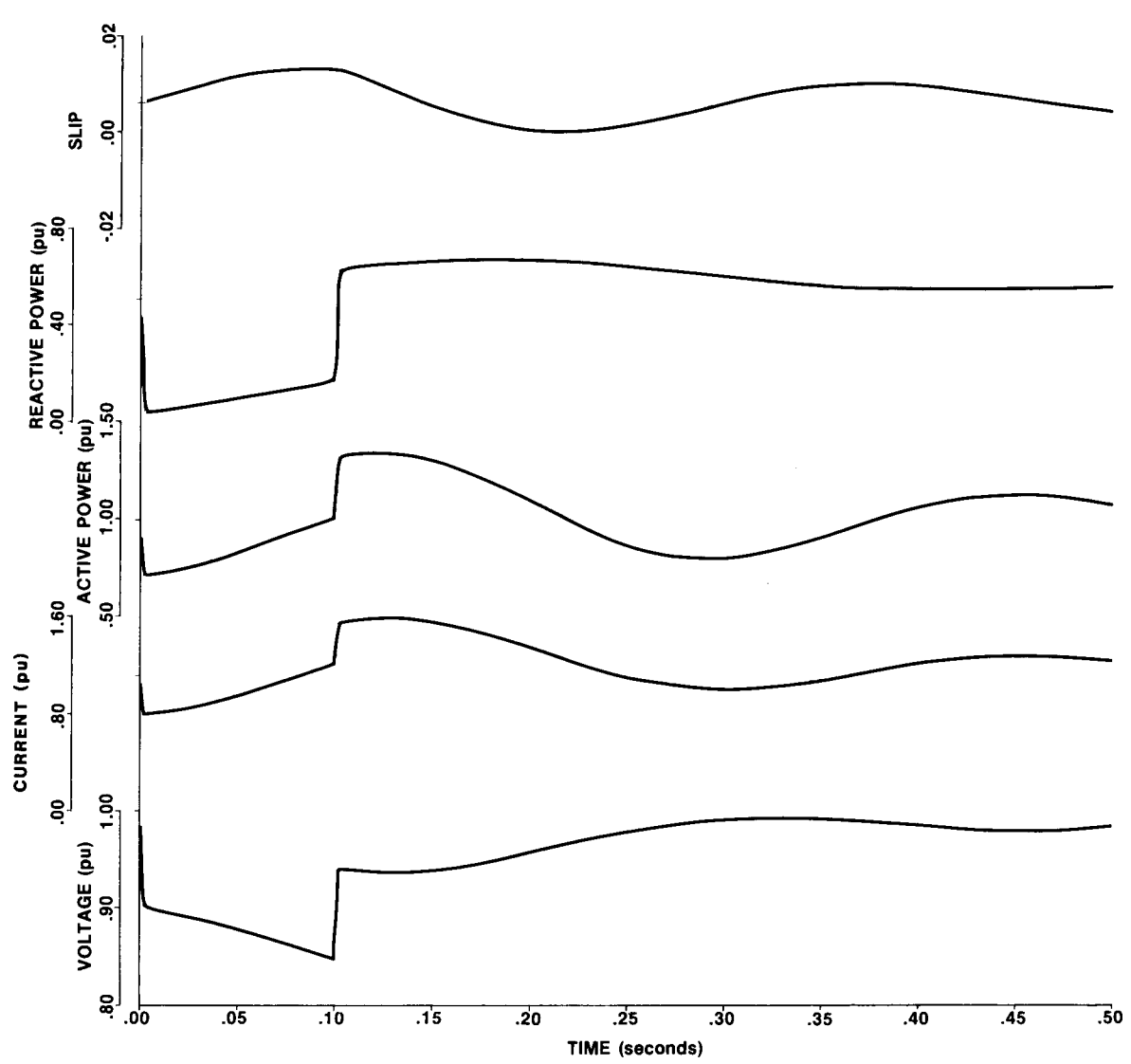


Figure 5-13. Transient response for 5500 hp motor, with rotor $p\psi$ terms; single motor to infinite bus system.

motor, Figure 5-13, there is less of a decay in motor terminal voltage during the fault due to the higher inertia constant and the higher X/R ratio of this machine. When the fault is cleared, there is a marked difference in the response with the interaction between the rotor electrical and mechanical systems producing an underdamped second order response in slip, active power, and terminal current. It has been previously noted that the larger horsepower motors tend to have lower design slips, higher transient X/R ratios in the rotor circuits, and produce noticeably underdamped responses to disturbances near the load area (33). It is likely that any study which involves a significant number of large motors at a single load area would require a detailed model of the motor to properly account for its affect on the system. This study did not determine the critical motor size above which a detailed model should be used.

The curve shown in Figure 5-14 shows the same transient disturbance for the 5500 HP motor with the exception that rotor electrical dynamics are eliminated by excluding the $p\psi$ terms in the rotor voltage equations. This gives a single state variable model involving only the rotor mechanical dynamics coupled with the classical steady-state electrical model. Comparing the two figures, it can be seen that neglecting the rotor electrical dynamics eliminates the underdamped response following the fault due to the interaction of the electrical and mechanical systems (34). The response of the single-state motor model also shows a markedly shorter settling time for the motor to reach steady-state after the fault.

The remaining curves, Figures 5-15 to 5-17, show motor P and Q plotted as a function of terminal voltage and correspond directly to the transient cases shown in Figures 5-12 to 5-14. These results indicate quite clearly that the steady-state curves which were generated for the induction motor do not adequately represent the motor under transient operating conditions ($\underline{14}$). The initial steady-state operating point is on the far right of these curves. The trajectory on these curves follow a clockwise direction with jumps or discontinuities when the fault is applied and removed. The time between each symbol on the curves shown in Figures 5-15 and 5-16 is 40 milliseconds.

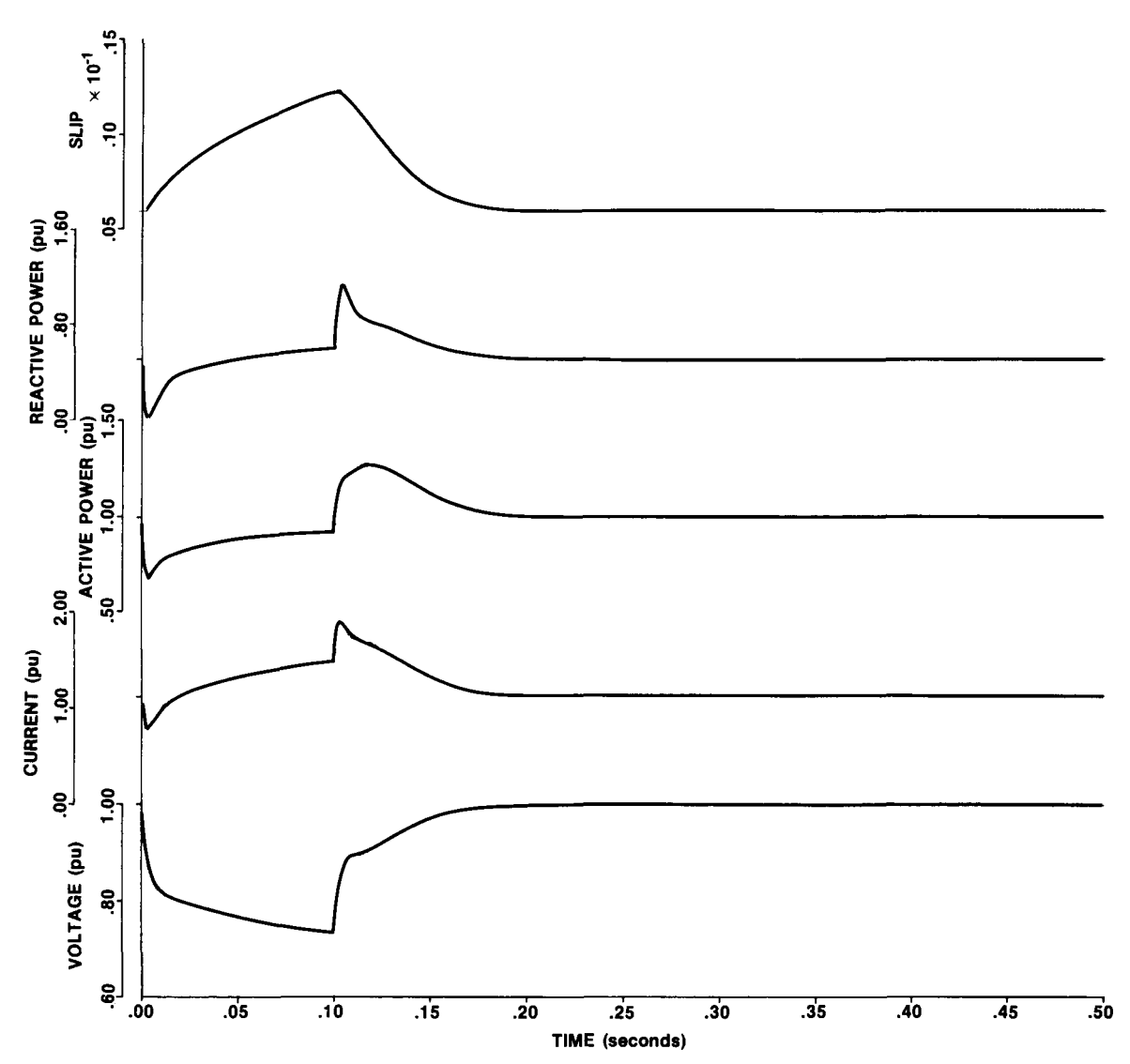


Figure 5-14. Transient response for 5500 hp motor, without rotor $p\psi$ terms; single motor to infinite bus system.

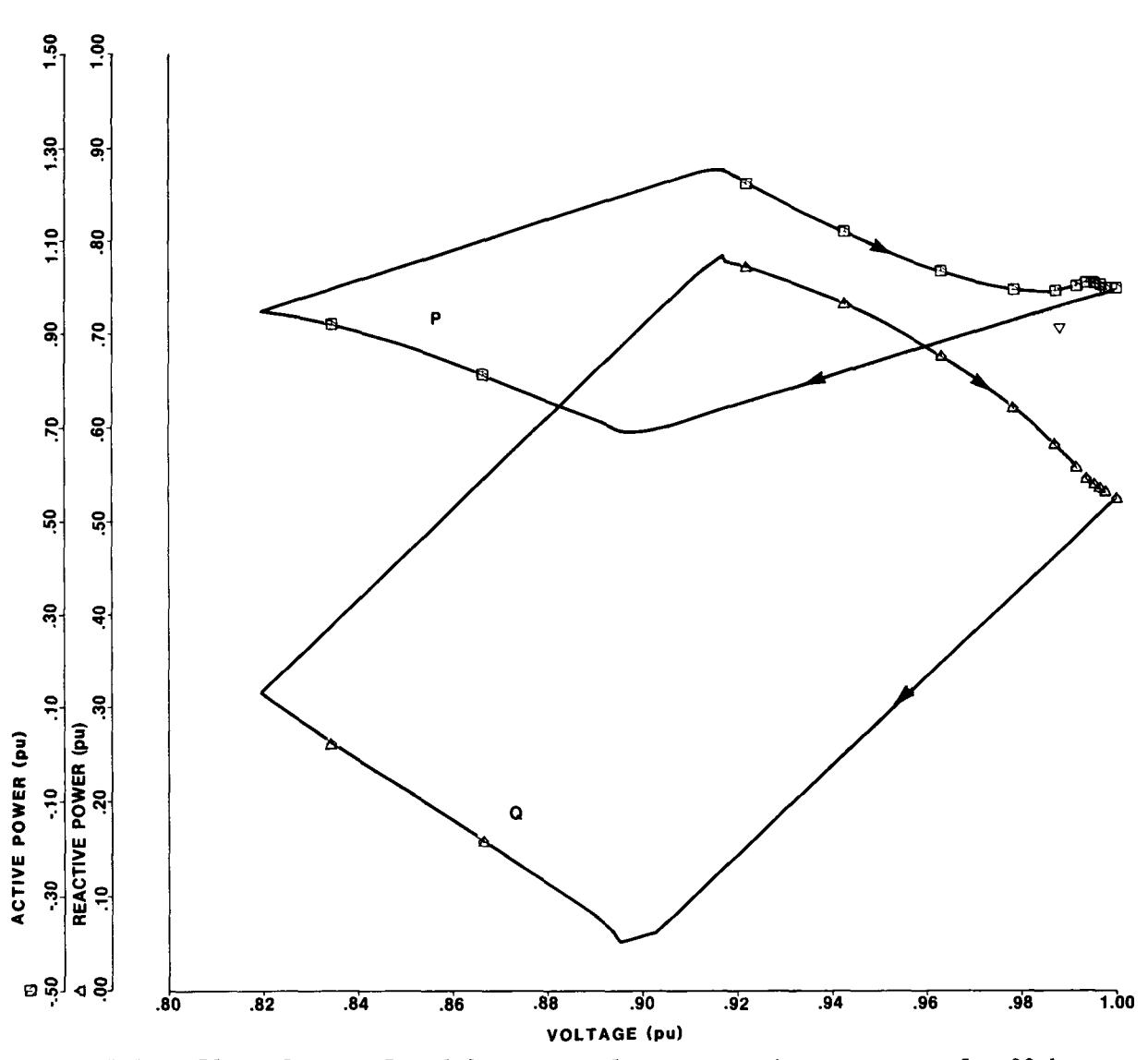


Figure 5-15. Plot of motor P and Q versus voltage; transient response for 30 hp motor (corresponds to Figure 5-12).

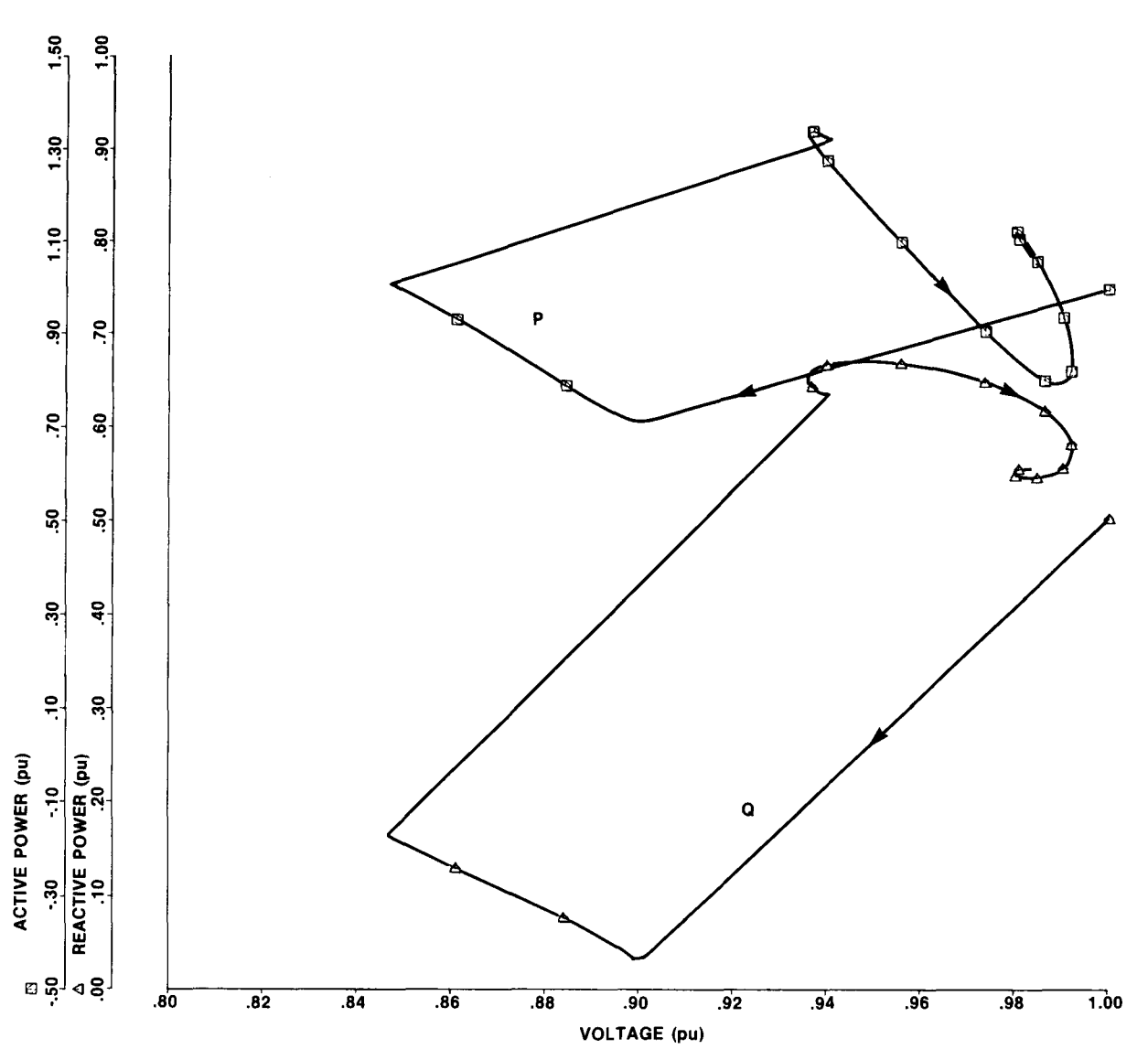


Figure 5-16. Plot of motor P and Q versus voltage; transient response for 5500 HP motor, with rotor p ψ terms (corresponds to Figure 5-13).

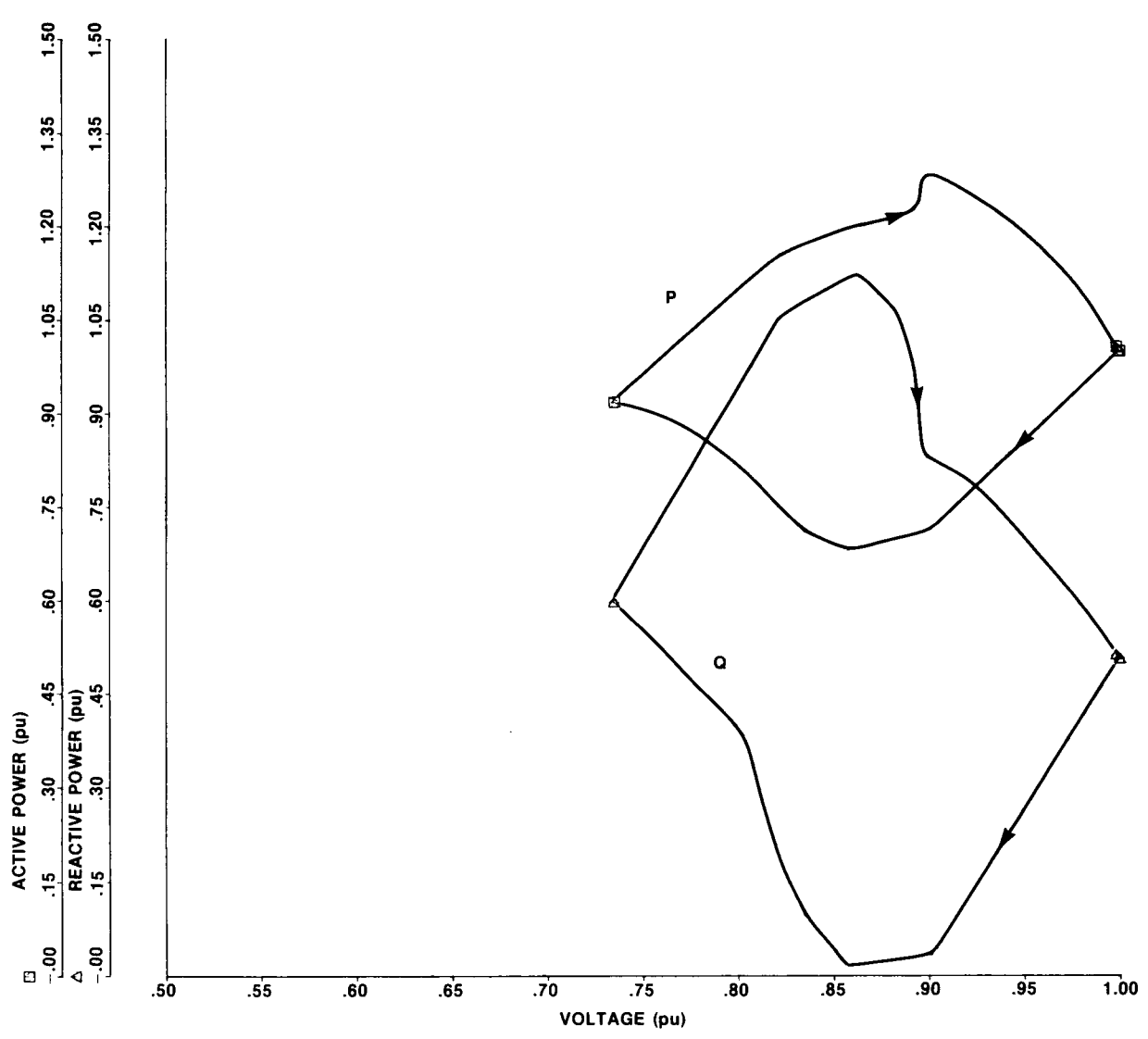


Figure 5-17. Plot of motor P and Q versus voltage; transient response for 5500 HP motor, without rotor p ψ terms (corresponds to Figure 5-14).

Section 6

REFERENCES

- 1. P.L. Dandeno and P. Kundur, "A Non-Iterative Transient Stability Program Including the Effects of Variable Load-Voltage Characteristics", IEEE Trans. Power Apparatus and Systems, pp. 1478-1484, Sept./Oct., 1973.
- 2. A.K. Kar and G.J. Berg, "System Performance Simulation with Improved Load Representation", IEEE Conf. paper C72 147-2 presented at 1972 Winter Power Meeting.
- 3. C. Concordia, Equipment Modeling-Loads, GE Report as part of the Advanced Power System Stability Seminar, 1979.
- 4. R.T.H. Alden and H.M. Zein El-Din, "Effect of Load Characteristics on Power System Dynamic Stability", IEEE Conf. paper A76-363-2 presented at PES Summer meeting, July 1976.
- M.H. Kent, W.R. Schmus, F.A. McCrackin and L.H. Wheeler, "Dynamic Modeling of Loads in Stability Studies", IEEE Trans. on Power Apparatus and Systems, Vol. 88, pp. 756-763, 1969.
- 6. G.J. Gevay and W.H. Schippel, "Transient Stability of an Isolated Radial Power Network with Varied Load Division", IEEE Trans. on Power Apparatus and Systems, Vol. 83, pp. 964-970, September, 1964.
- 7. C.B. Cooper, "Load Characteristics", A Symposium on Power System Dynamics presented at University of Manchester Institute of Science and Technology, September, 1973.
- 8. F. Iliceto, A Ceyhan, and G. Ruckstuhl, "Behavior of Loads During Voltage Dips Encountered in Stability Studies Field and Laboratory Tests", IEEE Trans. Power Apparatus and Systems, Vol. 91, pp. 2470-2479, Nov./Dec., 1972.
- 9. Ibid, discussion by R.H. Park.
- 10. V.S. Ramsden and N. Zorbas, "Prediction of Induction Motor Dynamic Performance in Power Systems", Proc. IEE, Vol. 115, No. 4, pp. 511-518, April, 1968.
- 11. M.Y. Akhtar, "Frequency Dependent Dynamic Representations of Induction Motor Loads", Proc. IEE, Vol. 115, No. 6, pp. 802-812, June 1968.
- 12. R.B. Squires of Gibbs and Hill, Inc. "Analytical Studies of Large Induction Motor Behavior during Bus Transfer", Paper presented at Protective Relay Engineers Conf., Texas A&M University, April 17, 1973.
- 13. D.G. Lewis and W.D. Marsh, "Transfer of Steam Electric Generating -Station Auxiliary Buses", Trans. AIEE, pp. 322-334, June 1955.
- 14. "System Load Dynamics Simulation Effects and Determination of Load Constants", IEEE Trans. Power Apparatus and Systems, Vol. 74, pp. 600-609, Mar./Apr., 1973.
- 15. C.C. Young, "Effect of Large Industrial Loads System Stability Problems," Paper presented to Conf. for Protective Relay Engineers, Texas A&M College, April 1960.

- 16. T.A. Lipo and A.B. Plunkett, "A Novel Approach to Induction Motor Transfer Functions", IEEE Trans. Power Apparatus and Systems, Vol. PAS-93, pp. 1410-1418, Sept/Oct. 1974.
- 17. M.M. Abdel Hahim and G.J. Berg, "Dynamic Single Unit Representation of Induction Motor Groups", IEEE Trans. Power Apparatus and Systems, Vol. PAS-95, pp. 155-165, Jan./Feb., 1976.
- 18. G.W. Staats, "Induction and Synchronous Motors Compared for System Stability", IEEE Trans. on Industry Applications, Vol. 1A-12, No. 5, pp. 470-473, Sept./Oct., 1976.
- R.H. Nelson, T.A. Lipo and P.C. Krause, "Stability Analysis of a Symmetrical Induction Machine", IEEE Trans. Power Apparatus and Systems, Vol. 88, pp. 1710-1717, Nov. 1969.
- 20. I. Racz, "Dynamic Behavior of Inverter Controlled Induction Motors", Proc. of 3rd Congress of IFAC, Vol. 1, pp. 4B1-4B7, June 1966.
- 21. A. Decarli, M. Murgo, and A. Ruberti, "Speed Control of Induction Motors by Frequency Variation", Proc. of 3rd Congress IFAC, Vol. 1, pp. 4C1-4C11, June 1966.
- 22. D.W. Novotny and J.H. Wouterse, "Induction Motor Transfer Functions and Dynamic Response by Means of Complex Time Variables", IEEE Trans. Power Apparatus and Systems, Vol. PAS-95, pp. 132-135, July/Aug. 1976.
- 23. W. Charlton, "Transfer and Weighting Functions for Variable Frequency Induction Motors", IEEE Trans. on Industry Applications, Vol. 1A-12, No. 5, pp. 474-478, Sept/Oct. 1976.
- 24. R. Stern and D.W. Novotny, "A Simplified Approach to the Determination of Induction Machine Dynamic Response", Paper A 77 123-3, Presented at the 1977 IEEE Winter Power Meeting.
- 25. P.C. Krause and C.H. Thomas, "Simulation of Symmetrical Induction Machinery", IEEE Trans. Power Apparatus and Systems, Vol. PAS-84, pp. 1038-1053, Nov. 1965.
- 26. Discussion by C.H. Thomas of paper by M. Riaz, "Analog Computer Representations of Synchronous Generators in Voltage-Regulation Studies", Trans. AIRIE, Vol. 75, p. 1182, December 1956.
- 27. P.C. Krause and A. Murdoch III, "Simplified Representations of Induction Machine Dynamics", 1975 IEEE Winter Power Meeting, paper C75 132-6.
- 28. D.F. Shankle, C.M. Murphy, R.W. Long, and E.L. Harder, "Transient Stability Studies I Synchronous and Induction Machines", Trans. AIEE, Vol. 73, Pt. III, pp. 1563-1580, February 1955.
- 29. S. Kalsi and B. Adkins, "Transient Stability of Power Systems Containing both Synchronous and Induction Machines", Proc. IEE, Vol. 118, No. 10, pp. 1467-1474, October 1971.
- 30. G.J. Berg and A.K. Kar, "Model Representation of Power System Loads", 1971 PICA Conf., Paper 71C26-PWR, pp. 153-162.

- 31. R.B. Adler and C.C. Mosher, "Steady-State Voltage Power Characteristics for Power System Loads", IEEE Conf. Paper 70 CP706-PWR.
- 32. B.M. Weedy and B.R. Cox, "Voltage Stability of Radial Power Links", Proc. IEE, Vol. 155, No. 4, pp. 528-536, April 1968.
- E.V. Larsen and A.S. Brower, "Hanford K-Area Boiler-Turbine-Alternator Modeling Project, ERDA Final Report 76-149, September 1976.
- 34. D.S. Brereton, D.G. Lewis, and C.C. Young, "Representation of Induction-Motor Loads During Power-System Stability Studies", Trans. AIEE, Vol. 76, Pt. III, pp. 451-461, Aug. 1957.

APPENDIX A
PARAMETERS FOR SYSTEM STUDIES

Expressed in per unit on the machine ratings, the generator parameters are:

The saturation relation for each unit is detailed in the following table:

Ψ ag	$^{\mathrm{X}}$ ad $^{\mathrm{I}}$ fd
0.8	0.8
0.9	0.93
1.0	1.088
1.05	1.173
1.10	1.289
1.15	1.449
1.20	1.687

No governor action or prime mover system was represented, and the input torque was held constant at a level corresponding to the steady-state operating points shown in the load flow.

The excitation system used with each generator was a 2.0 response ratio, high initial response unit. The parameters for the IEEE Type 1 model are:

For the conventional 0.5 response ratio exciter, used in the study relating to Figure 3-4, the parameters are

The line and transformer data for the two machine system are as follows (on a 3000 MVA base):

Generator Step up Transfomers

$$r = 0, x = 0.10$$

Bus 4 - 5

Transmission Lines

Bus 2 - 3
$$r = .02$$
, $x = .20$, $B/2 = .10$
Bus 3 - 4 $r = .015$, $x = .15$, $B/2 = .10$

Distribution Transformers

Bus
$$3 - 7$$
 $r = 0, x = 0.10$

Bus 4 - 8

The induction motor data expressed in per-unit on a base of the motor ratings is:

	30 HP	5500 HP
r	.025	.00572
$\mathbf{x}_{\ell 1}$.0864	.1273
X _m	2.92	3.75
r ₂	.0153	.00522
$X_{\ell 2}$. 149	.1095
H	1.0	1.0 .

The inertia values given include a typical load inertia, and the values of magnetizing reactance given in the table are for no load operation at rated terminal voltage. The relationship for saturation in the magnetizing path is detailed in the following table of per-unit values:

		Ψ m
MMF	30 HP	5500 HP
0.8	0.8	0.8
1.0	0.88	0.925
1.2	0.95	1.02
1.4	0.98	1.08
1.6	1.03	1.14
1.8	1.07	1.18